Russian Chemical Reviews **82** (7) 597 – 615 (2013) © 2013 Russian Academy of Sciences and Turpion Ltd

DOI 10.1070/RC2013v082n07ABEH004394

Extreme states of matter on the Earth and in the cosmos: is there any chemistry beyond the megabar?

V E Fortov, V B Mintsev

Contents

I. Introduction 597
II. Generation of extreme states of matter 598
III. Physicochemical properties of matter under extreme conditions 604

Abstract. The results of studies of thermodynamic, transport and optical properties of highly compressed matter at high pressures and temperatures are analyzed. Experimental methods for cumulation of high energy density, generation of strong shock waves and rapid diagnostics of high-energy plasma are considered. The effects stimulated by compression — pressure-induced ionization, plasma phase transitions, deformation of coupled states, plasma transparentization and structure transformation are discussed. The bibliography includes 107 references.

I. Introduction

In recent years, considerable attention of researchers has been drawn to studies of the state of matter under extreme conditions, *i.e.*, extremely high pressures and temperatures.[1–5] This is related, first of all, to the necessity to invade new domains of substance phase diagrams and to obtain, under laboratory conditions, the exotic states of substances that gave rise to the Universe as a result of Big Bang, which is of high value for gaining knowledge and for the formation of modern views on the surrounding world. This brings about exceptionally interesting and important questions of how high pressures and temperatures affect the chemical behaviour of a substance, in particular, how the chemical reactivity changes, what new chemical effects can be expected, what is the role of chemical processes in the formation of the modern world.

The science of extreme states of matter and chemistry have always been intertwined. Indeed, the use of chemical energy of high explosives (HE) to encroach the area of extreme parameters has long been a separate line of research.[1,6] In Russia, it appeared in the 1930s at the Leningrad Physical Technical Institute headed by A F Ioffe and was further developed at the Institutes of Chemical Physics and Problems of Chemical Physics (Chernogolovka). Outstanding scientists such as N N Semenov, Yu B Khariton, Ya B Zel'dovich and others worked at these institutes; their works pioneered this field of research and, what is more important, they formed the foundation of a scientific school engaged in investigations of matter under these unusual conditions.

The dynamic methods of generation of high pressures and temperatures based on the use of chemical energy of HE not only allowed entering the region of extreme parameters but also made the lifetimes of investigated subjects ($\sim 10^{-9}$–10^{-6} s) to be sufficient for identification of fast processes.[1–7] There are only three ways to gain high pressures and temperatures at researchers' disposal — compression, heating and exposure to a strong electromagnetic field, which induce a crucial rearrangement of the electronic structures of, first, outer and then inner electron shells, which sharply changes the reactivity of the substance. Indeed, at low pressures and temperatures, a substance has highly diversified properties, which we can observe every day under ambient conditions.[2] The physical, chemical, structural and biological properties of a substance depend on the arrangement and characteristic features and details of occupation of the electronic levels of atoms, ions and molecules, which ultimately determine the amazing abundance of forms and manifestations of living and nonliving nature on the Earth. Study of the variation of these key characteristics at high pressures and temperatures allows one to follow also the variation of physicochemical properties. Therefore, currently the question of how a substance would behave at a pressure of $\sim$1 Mbar (1 000 000 atm) and higher acquires a new meaning. During the last 10–15 years, results were obtained that contradict what had been expected in the 1980s.[1]

This review considers the behaviour of the electronic structures of substances under extreme conditions, new effects that can be expected and the methods that can produce these states under laboratory or quasi-laboratory conditions. Indeed, apart from various laboratory methods for attaining high temperatures, there is the cosmos. As

V E Fortov Joint Institute for High Temperatutes, Russian Academy of Sciences, ul. Izhorskaya 13, bd. 2, 125412 Moscow, Russian Federation. Tel. (7-495) 484 16 38, e-mail: fortov@ihed.ras.ru
V B Mintsev Institute of Problems of Chemical Physics, Russian Academy of Sciences, prosp. Akad. Semenova 1, 142432 Chernogolovka, Russian Federation. Tel. (7-496) 522 56 36, e-mail: minvb@icp.ac.ru

Received 5 April 2013
Uspekhi Khimii **82** (7) 597–615 (2013); translated by Z P Svitanko

Academician Ya B Zel'dovich metaphorically said, the Universe is 'accelerator for the poor', which, without requiring multibillion expenditures for the construction of experimental devices, provides information on strongly compressed and heated media that arise in the supernova centres upon explosions, in neutron stars, black holes, *etc*. Thus, we obtain a complete view of where matter and all chemical elements come from. Today it is known for certain and generally accepted [8,9] that, while moving from hydrogen — the most naturally abundant element — to iron and nickel, it is possible to obtain the whole chain of chemical elements by thermonuclear fusion reactions; however, the further elements from iron to uranium arise in the supernova explosions. Therefore, it can be said that heavy elements result from operation of an inertial confinement fusion reactor.

The interest in the extreme state physics has always been rather high due to the natural striving of people to go ahead, reach the margin of the unknown and understand what is situated beyond this margin, and to work with record high parameters. Humans as biological objects live at room temperature and at a pressure of about 1 atm. However, this is an exception, as most part of the visible matter occurs in highly compressed and heated state, *i.e*., under extreme conditions. Therefore, the astrophysical aspects of the science of extreme states of matter provoke particular interest. Indeed, according to modern estimates, $\sim$95% of the mass of the Universe (without considering the 'dark matter') is composed of matter at superhigh pressures and temperatures in common and neutron stars, pulsars, black holes, giant planets and exoplanets.[1–5] The limiting pressures of laboratory plasma still differ from the maximum astrophysical values by 20–30 orders of magnitude; however, this gap rapidly decreases, and the physical processes in laboratory and in outer space often demonstrate remarkable diversity and, simultaneously, close analogy, which indicates at least that the physical principles of behaviour of matter are the same over a very broad range of densities ($\sim$42 orders of magnitude) and temperatures (up to 10^{13} K).

It is important that in addition to fundamental problems, the range of technological problems related to the physics and chemistry of the extreme states of matter is continuously extending. These states determine the operation of inertial confinement pulsed fusion reactors, high-power magnetic explosion and magnetohydrodynamic generators, power installations and rocket engines with gas core nuclear reactors, plasmochemical and microwave reactors, plasmotrons and high-power optical and X-ray radiation sources. In power installations of the future, highly compressed and heated plasma will serve as the working body, like steam used in modern thermal electric power stations.

In recent years, vigorous theoretical and experimental studies have provided new and, what is important, reliable data about thermodynamic, structural, gas dynamic, optical, electrophysical and transport properties of substances under extreme conditions. Data on the chemical processes at high pressures and temperatures are much more scarce; however, the revealed general trends are suitable for predicting the whole picture.

In turn, as Academician A L Buchachenko emphasized,[10] 'Modern chemistry is intensively expands its horizons and actively invades the areas that have been of no interest for the 'old' chemistry. It moves faster and faster from 'familiar' regimes and conditions towards extreme, non-classical and even exotic conditions, *i.e*., superhigh pressures and shear deformations, strong electric and magnetic fields, high-intensity light, gravitational, acoustic and microwave fields and so on.'

II. Generation of extreme states of matter

How can high pressures and temperatures be realized in the laboratory? In recent years, two clear-cut trends have formed — one using static and one using dynamic methods for generation of extreme states.[1,6] The experimental installations used for this purpose are quite diverse: diamond anvils for static compression of substances, powder and light-gas launching devices (guns), explosive-driven generators of high-intensity shock waves, devices for electrical explosions magnetocumulative generators, lasers, pulsed power generators of high-intensity electric current pulses, charged particle accelerators and possible combinations thereof.

A considerable progress in static pressures was achieved in the early 1980s with the advent of diamond anvil experimental technique (Fig. 1).[11,12] In these installations, two diamonds faceted in a special way compress thin (10–100 μm) planar layers of a substance to the highest possible megabar pressure, the upper limit of which is determined by the maximum strength of diamond ($\sim$0.5–1.0 Mbar). In some experiments, the compressed matter is heated by laser radiation,[13] or the material compressed by diamond anvils serves as the target for the subsequent compression by laser shock waves.[14] Owing to the infinite time of static compression, it is possible to use various diagnostic means, including spectroscopy, and to perform X-ray diffraction analysis using kiloelectron-volt X-ray and synchrotron radiation. These experiments gave quite a lot of useful information on the mechanical properties, thermodynamics and phase transformations of geophysical objects under conditions extreme for the Earth: $P \approx 0.1-3.6$ Mbar, $T \approx 10^3-6\times10^3$ K.

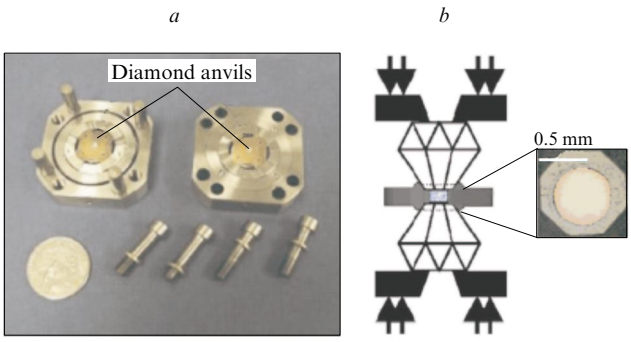


Figure 1. Photographic image (*a*) and schematic (*b*) of the installation for static compression by diamond anvils.[11]

Further movement along the scale of high energy densities is associated with switching to dynamic methods [3–5,15–22] based on the pulse energy cumulation in the sample being investigated by means of high-intensity shock waves, electromagnetic or corpuscular radiation of various natures. The plasma temperature and pressure

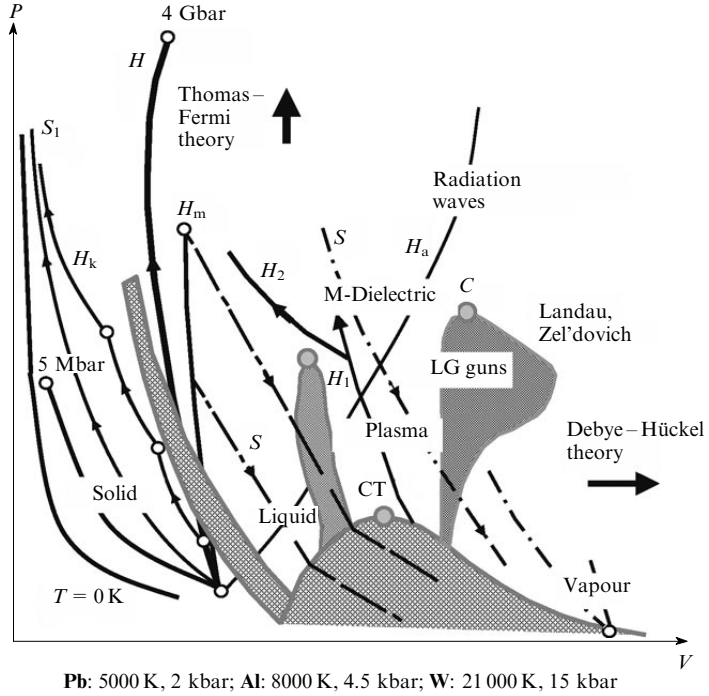


Figure 2. Thermodynamic paths of the dynamic investigation methods.[4]
The domains of the parameters where the classical Thomas – Fermi and Debye – Hückel theories operate are marked and also the domain of existence of the possible plasma phase transition predicted by Landau and Zel'dovich with critical point *C*. *S* and S_1 are expansion and compression adiabatic curves; *H* is shock compression of aluminium with the maximum achieved pressure of 4 Gbar (400 TPa); H_1 and H_2 is gas compression by incident and reflected shock waves; H_m and H_a is compression of massive and porous samples of condensed materials by intense shock waves; H_k is multistage (quasi-isentropic) compression; CP is critical point; LG guns corresponds to the domain of parameters reachable using light-gas guns. At the bottom, critical point parameters for some metals are given.

substantially exceed the thermomechanical limits of the structural materials forming the installations, and this restricts the characteristic lifetime of plasma, which is determined by the dispersion dynamics of the target and is equal to $\sim 10^{-10} - 10^{-5}$ s. In the dynamic approach, there are no fundamental limitations on the maximum energy densities and pressures developing in the target, these values being limited only by the power of the energy source.

High-intensity shock waves arising as a result of nonlinear hydrodynamic phenomena in a substance as it moves due to pulse energy release is the most widely used tool for creating high energy density.[1, 18 – 20] The key role is played by the shock wave, a thick compression shock, in which the kinetic energy of the incident flow is converted to the thermal energy of compressed and irreversibly heated plasma.

Currently, the shock-wave technique plays a key role in the high energy density physics; this makes it possible to develop megabar- and gigabar-range pressures. The achieved range of maximum dynamic pressures is six orders of magnitude higher than the pressure developed upon a bullet impact, three orders of magnitude higher than the pressure at the centre of the Earth and is close[16, 21] to the pressure in central parts of the Sun or in inertial thermonuclear fusion targets. Such exotic states of matter were involved in the origination of the Universe several seconds after the Big Bang.[5, 23, 24] In a certain sense, it can be considered that by successively increasing pressure and temperature in dynamic experiments, we move backwards along the time axis, thus approaching the instant of origination of the Universe — Big Bang.[1]

A shock wave not only compresses but also heats matter to high temperature, which is especially important for the generation of plasma, the ionized state of matter. The shock compression of a material in the solid or liquid initial state gives rise to the state of non-ideal degenerate (Fermi statistics) and classical (Boltzmann statistics) plasma behind the shock wave front, the plasma being compressed to the highest pressures of ~ 4 Gbar and heated to about 10^7 K,[16, 21] where the internal energy density of the plasma is comparable with the nuclear energy density. These conditions are similar to the conditions where the equilibrium radiation energy and pressure start to play a noticeable role in the overall thermodynamics and dynamics of these high-energy states (Fig. 2).

To decrease the irreversible heating effects, it is expedient to use compression of a substance by a sequence of incident and reflected (H_k) shock waves;[1, 15, 25, 26] as a consequence, this becomes more similar to 'soft' isentropic compression and gives much higher compression ratios (10 – 50 times) and lower temperatures (~ 10 times) in comparison with a single-stage shock-wave compression. Multiple shock compression was successfully used for experimental investigation of pressure-induced plasma ionization[1, 15, 25, 26] and substance dielectrization[27] under megabar pressures. The quasi-adiabatic compression S_1 was also implemented in the highly symmetric cylindrical explosive compression of hydrogen and inert gases (Fig. 3). Experiments on soft adiabatic plasma compression by a megagauss magnetic field were discussed in publications.[28, 29]

In the other limiting case, where it is necessary to obtain high-temperature plasma, it is expedient to perform the shock-wave compression of lower-density (compared with solids) targets — porous metals (H_m)[1, 3, 17 – 20, 30] or aerogels (H_a)[31] (see Fig. 2). This sharply increases the irreversibility of shock compression and thereby increases the entropy and temperature of the compressed state.

The shock compression of noble gases and saturated alkali metal vapour by incident (H_1) and reflected (H_2) shock waves (see Fig. 2) can be used to study plasma with electrons obeying the Boltzmann statistics in the region of developed thermal ionization.[1 – 4, 17, 25] A characteristic feature of the shock wave technique is that it is suitable for

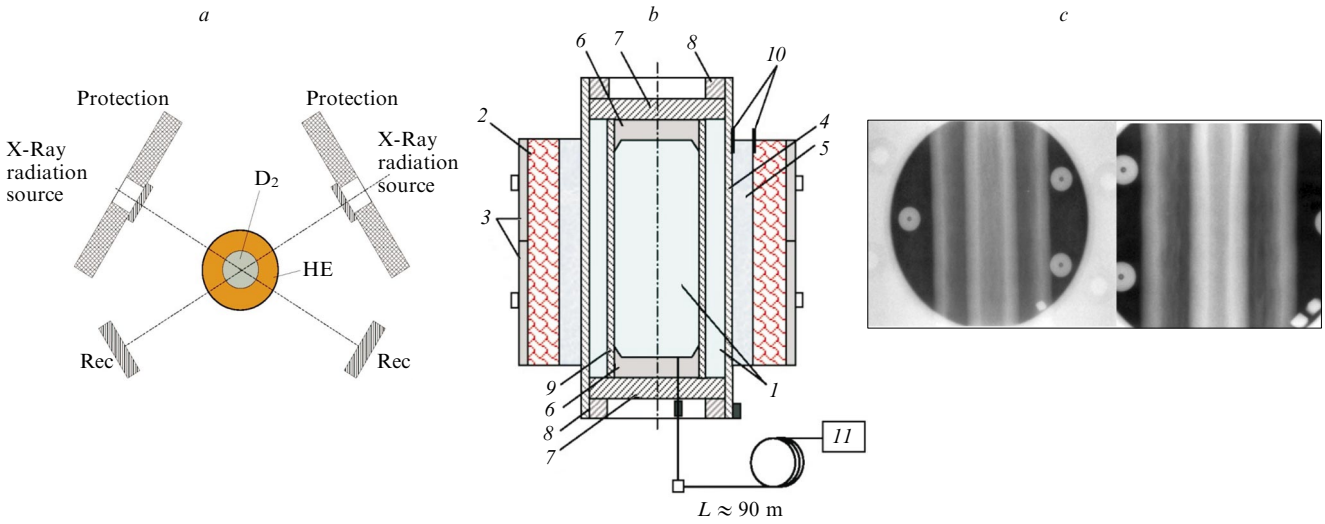


Figure 3. Layout (*a*), cross-section of the chamber of cylindrical explosion device for quasi-adiabatic plasma compression (*b*) and plasma X-ray diffraction patterns at different time instants (*c*).[26]
HE is high explosive, Rec is recorder; (*1*) deuterium gas, (*2*) CE block, (*3*) focusing system, (*4*) outer sheath, (*5*) organic glass, (*6*) insets, (*7*) blind flanges, (*8*) screw nuts, (*9*) inner sheath, (*10*) electric connections, (*11*) gas source.

developing high pressures and temperatures in compressed media, whereas the low-density domain in the $P-V$ diagram (including the boiling curve and the critical point neighbourhood) is inaccessible for this technique.[1–4] The intermediate states of plasma can be studied by isentropic expansion technique based on plasma generation by adiabatic expansion (S) of condensed material precompressed and irreversibly preheated in a high-intensity shock wave front.[1–4] This procedure was used for the first experimental study of the high-temperature regions of the boiling points curves, near-critical states and metal–dielectric transition regions for a large number of metals (for details, see the publications [1–4, 32, 33]).

The major physical information about the plasma behaviour at pressures up to 10–15 Mbar is gained using the technique of high-intensity shock waves excited by collision of metallic liners (strikers) accelerated to velocities of several kilometres per second with a target made of the substance to be studied. We will not describe in detail the liner acceleration methods and diagnostic means — they are subjects of detailed reviews and monographs (see, for example,[1–4, 15–19, 25, 34, 35]). Note only that shock-wave experiments allow comprehensive measurements of the physical properties of plasma. For determining the equation of state, electrocontact and optical recording of the temporal intervals of motion of shock-wave discontinuities and contact surfaces are carried out; pyrometric, spectroscopic, proton diffraction, X-ray diffraction and adsorption measurements are performed using pulse X-ray and synchrotron radiation sources; laser interferometric measurements, recording of low- and high-frequency Hall conductivity and detection of piezo- and magnetoelectric effects are carried out. Unique information was gained from a study of mechanical properties of shock-compressed media such as elastoplastic properties, spalling phenomena, polymorphism, viscosity, destruction and fragmentation.[36] A lot of unexpected results were obtained in a study of the chemical reactions and kinetics of physicochemical transformations in shock and detonation waves.[36]

In the USA, most popular are powder and light-gas launching units (guns),[15] while in the USSR explosive-driven launching units were preferred.[34]

In order to increase the launching speed and, hence, pressure of the shock-compressed plasma, original gas-dynamic methods are used. The 'gradient' cumulation technique [30, 37] is based on the successive increase in the speed of strikers in planar alternating layers of heavy and light materials (Fig. 4). This technique is not related to

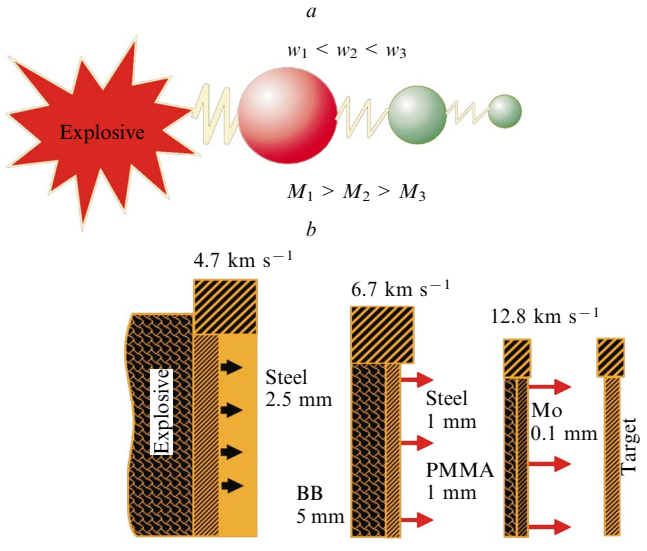


Figure 4. Illustrations of the gradient cumulation principle (*a*)[37] and the action of explosion three-stage 'layer cake' (*b*).[30, 34]
w_i and M_i are the bead velocity and mass, respectively; PMMA is polymethyl methacrylate.

geometrical energy focusing and, therefore, it possesses a higher stability of acceleration and compression processes (as compared with spherical compression). The explosive three-stage 'layer cake'[30,34] constructed in this way accelerated a 100-micrometre molybdenum striker to 5–14 km s^{-1}. The impact of such striker excites, in the target plasma, a planar shock wave or a series of reverberating shock waves with a megabar-range amplitude pressure. The geometric parameters of these experimental devices are selected in such a way as to eliminate the distorting effects of the side and rear depression waves and to ensure the one-dimensional and stationary nature of the gas-dynamic flow in the recording area.

It is of interest that the kinetic energy of a metallic striker that moves at a speed of 10 km s^{-1} is close to the kinetic energy of a proton beam in the cyclotron accelerator of the Fermi National Accelerator Laboratory (Illinois, USA). This high kinetic energy in shock-wave experiments generates a strongly compressed plasma at high temperature just as the collision of relativistic ions produces a quark-gluon plasma with very high energy density.

To increase the shock compression parameters, explosion generators of counter-propagating shock waves were used in some experiments (Fig. 5) in which the material being investigated was loaded on both sides by synchronous impacts of steel strikers symmetrically accelerated by explosive charges.[38,39]

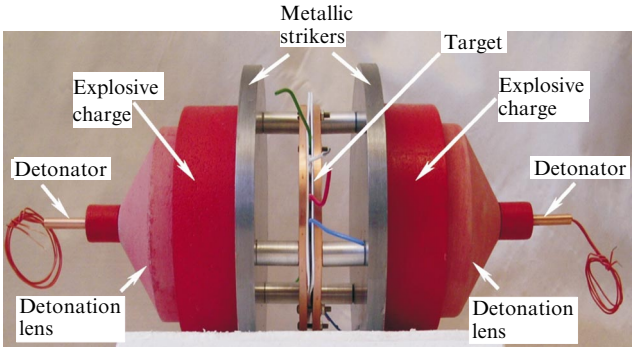


Figure 5. Photographic image of an explosion generator of counter-propagating shock waves.[38,39]

Especially precise spherical explosion generators of high-intensity shock waves (Fig. 6) were designed in the USSR to study the thermodynamic properties of materials at pressures up to 10 Mbar.[17–19,34,40] Using the geometric cumulation effects, during centripetal motion (implosion) of detonation products and hemispherical shells, in devices weighing ~100 kg with energy release of ~300 MJ, metallic strikers were accelerated to ~23 km s^{-1}.

Experimental data on the thermodynamic properties of non-ideal deuterium plasma[40–42] obtained upon cylindrical and spherical shock-wave compression are shown in Fig. 7 where they are compared with the results of laser[43] and electrodynamic experiments.[44] According to estimates, in these experiments, shock-compressed plasma is strongly non-ideal (the non-ideality parameter $\Gamma > 1$) and has developed ionization and partial degeneracy. It can be seen that non-ideal plasma models[25,30,45] adequately describe the data of explosion and electrodynamic experiments.

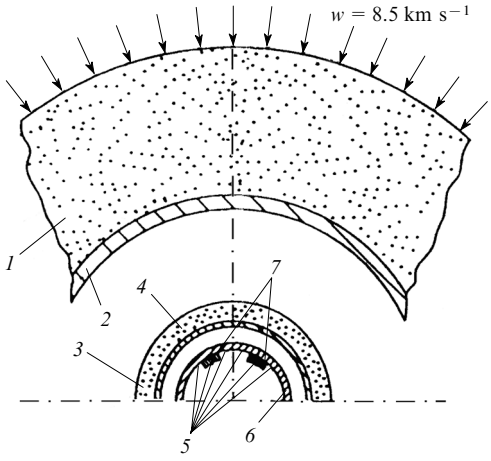


Figure 6. Schematic of the explosion generator of spherically converging intense shock waves.[17,34]
(*1*, *3*) First- and second-cascade explosive charges; (*2*, *4*) first- and second-cascade sheaths; (*5*) electric contact sensors; (*6*) screen (Fe); (*7*) samples.

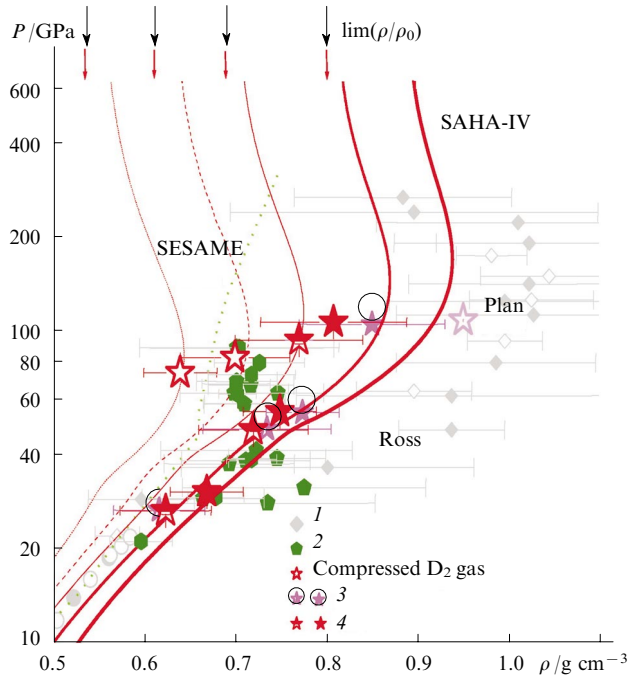


Figure 7. Shock-wave compression of deuterium plasma.[41–44]
The arrows mark the SAHA-IV-calculated limited compressions of deuterium for different initial densities corresponding to the initial conditions of sphere experiments;[40] Ross, SESAME and SAHA-IV are theoretical models;[1,6] Plan is planned experiment; experimental data [1] obtained using the NOVA laser (*1*), Z-pinches (*2*), explosive spherical systems with solid D_2 (see Refs 1 and 40) (*3*) and solid and liquid D_2 (see Refs 1 and 42) (*4*).

In more stable conical explosion generators, cumulation effects were used with irregular (Mach) convergence of cylindrical shock waves (Fig. 8). The combination of irregular cylindrical cumulation and 'gradient' cumulation effects gave rise to a shock wave in copper with a

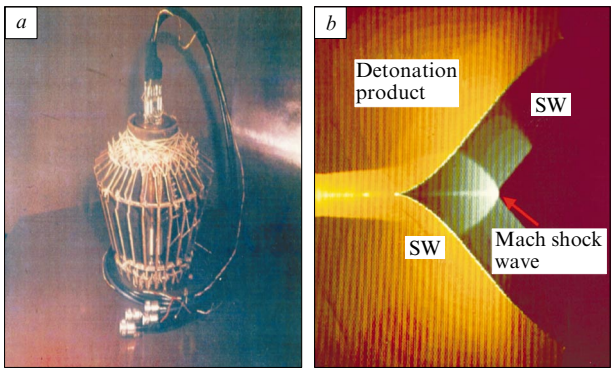


Figure 8. Photograph (*a*) and results of two-dimensional hydrodynamic calculation of a conical explosion generator of Mach shock waves (*b*).[46]
SW is shock wave.

~20 Mbar amplitude, which is close to the pressure in the near zone of a nuclear explosion.

Pulsed power (10^5–10^7 A) electronic devices for obtaining high energy densities in a substance are used in various experiments. Electrical energy may induce direct pulsed Joule heating (electrical explosion) of conductors [1] or magnetodynamic compression and heating of plasma structures. This stored energy can be used to produce intense bursts of soft X-ray radiation (with radiation temperature of 200–300 eV), which then generate intense shock or radiation heat waves, or for electrodynamic generation of shock waves and for electrodynamic acceleration of metallic liners.

Currently, the highest plasma parameters have been attained in terawatt-range Z-pinches in which the electric energy accumulated in capacitors after the appropriate sharpening of the electric pulse shape is used for electrodynamic plasma acceleration followed by focusing of the plasma kinetic energy on a cylinder axis.[47,48] The most interesting application of this installation is related to the electrodynamic generation of intense shock waves:[44] a high-intensity (~20 MA) electric current pulse induces electrodynamic acceleration of a metallic striker to a speed of ~45 km s^{-1}; when the striker hits the target, megabar-range pressure is generated. This brings about an interesting opportunity of shock-free 'soft' compression of hydrogen targets to a ~3 Mbar pressure by controlling the current parameters.

In experiments conducted at the 'Angara' installation,[49] a plasma xenon liner was accelerated under the action of ~4 MA pulsed current to a velocity of ~500 km s^{-1}. Highly symmetrical impact of this liner on the surface of a highly porous cylindrical target excited a radiation heat wave, which emitted soft X-ray radiation with a temperature of ~100 eV. This intense X-ray radiation from the cylindrical cavity was used for highly symmetrical generation of planar shock waves with a pressure amplitude of ~5 Mbar for the excitation of radiation heat waves propagating at ~100 km s^{-1} and for acceleration of metallic strikers to 10–12 km s^{-1}.

The impetuous development of laser technology resulted in the possibility of generation of ultrashort (nano-, pico-, femto- and attosecond) laser pulses and in switching (Fig. 9, see also Tables 3, 4 in monograph [1]) of laser facilities, both existing and being constructed, to the peta- and zetawatt power ranges.[5,50] This provided a broad range of power densities up to the currently uttermost high values of $22-10^{23}$ W cm^{-2}. The interaction of intense laser radiation with matter is under vigorous research and has been described in detail in dedicated papers.[51–55] The most

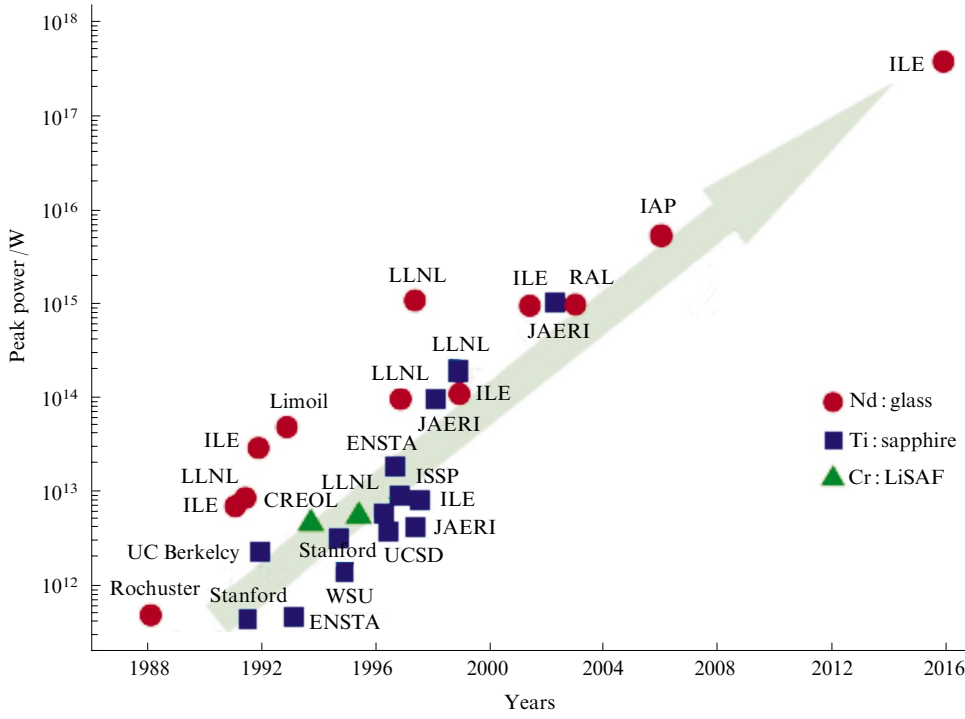


Figure 9. Powers of laser installations.[1]

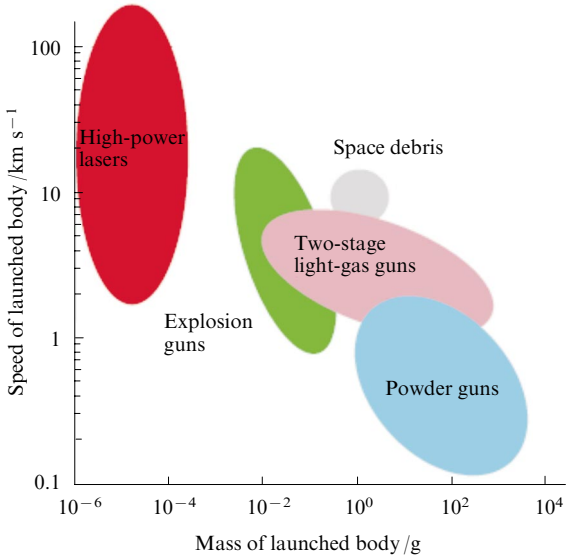


Figure 10. Possibilities of high-speed launching methods.[1]
For comparison, the characteristic speeds and particle masses of space debris are given.

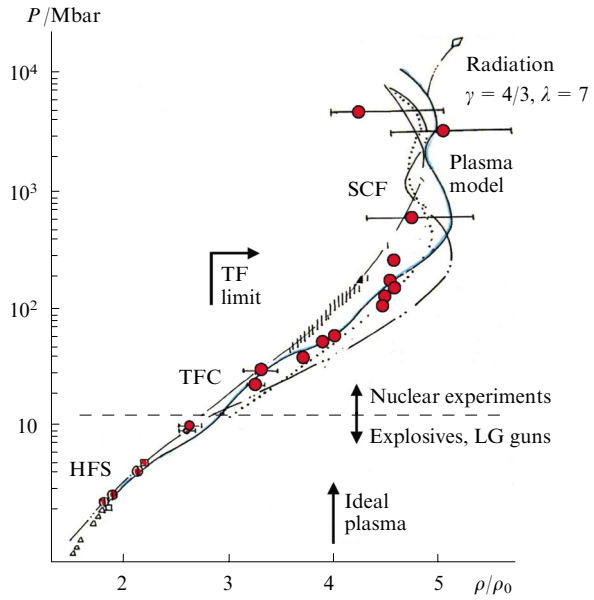


Figure 12. Shock-wave compression of aluminium to gigabar pressures.[16, 21, 58]
Theories: Hartree – Fock – Slater (HFS), Thomas – Fermi with corrections (TFC), Thomas – Fermi (TF), self-consistent field (SCF); ρ_0 is the initial density.

powerful laser facility NIF [56, 57] has an energy of $\sim$2 MJ in 192 beams, thus providing conditions close to the conditions of thermonuclear fusion ignition. Installations of this type make it possible to approach experiments with gigabar pressure range shock waves and thus to move towards quasi-classical description of matter [2] and to study the plasma flow under conditions of developed radiation effects.

The possibilities of various launching methods are illustrated by Fig. 10.

The record-high plasma energy densities were obtained in the near zone of nuclear explosion. Some physical implementations of such experiments were reported [16, 21, 34, 35, 58, 59] (Fig. 11). Experimental data concerning the shock-compressed aluminium plasma are shown in Fig. 12 where the highest points correspond to the highest parameters achieved on the Earth.[58] The internal energy density of this plasma is $\sim 10^9$ J cm^{-3}, which is close to the energy density of nuclear matter, and the pressure $P \approx 4$ Gbar is close to the pressure in the inner parts of the Sun. Under these conditions, plasma is non-degenerate and 12 times ionized, and the non-ideality parameter is rather low ($\Gamma \approx 0.1$), which experimentally illustrates the statement that the physical properties of plasma are simplified in the ultrahigh energy density limit.

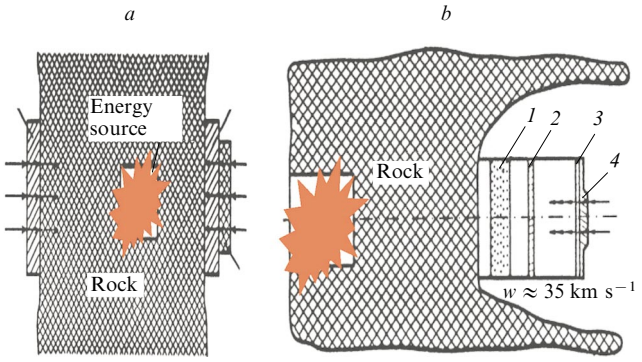


Figure 11. Experimental design for generation of intense shock waves in the near zone of a nuclear explosion.[16, 21, 35, 59]
(*a*) Reflection method, (*b*) determination of the shock compressibility of iron by the retardation method; (*1*) plastic foam, (*2*) striker (Fe), (*3*) screen (Fe), (*4*) target, $w \sim 35$ km s^{-1}.

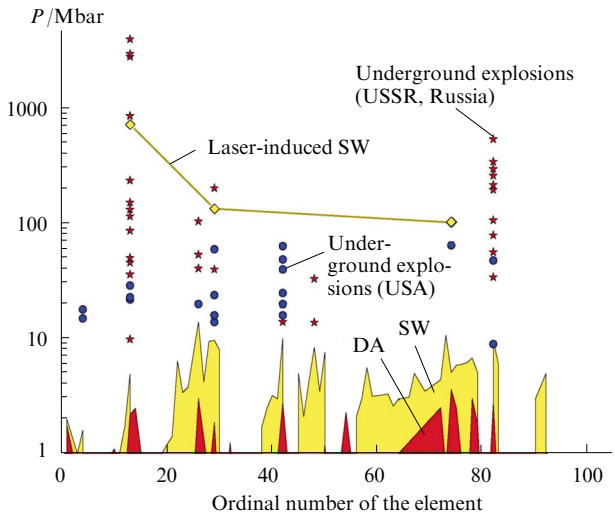


Figure 13. Characteristic pressures implemented in experiments on the Earth.[1]
DA is the static diamond anvil method, SW are shock waves from light-gas guns and chemical explosives.

The pressure values achieved to date under controlled conditions using shock waves and diamond anvils are given in Fig. 13. It can be seen that going to >10 Mbar values requires the use of non-traditional methods of shock-wave generation, first of all, laser methods. Those interested in ultrahigh pressure issues may refer to some publications.[1, 3, 15, 20, 33, 34]

III. Physicochemical properties of matter under extreme conditions

What happens to chemistry at megabars? In order to answer this question, it is necessary first of all to consider the behaviour of the electronic states, which determine the physical and chemical properties of substances, following the variation of pressure and temperature. The description of coupled electronic states is crucially simplified at extremely high pressures ($P \approx e^2/a_B^4 \approx 300$ Mbar, where a_B is the Borh radius of the electron) or temperatures ($T \sim$ Ry $\approx 10^5$ K) where the electronic shells are 'collapsed' and their properties are described in terms of the quasi-classical approach to the self-consistent field method — the Thomas – Fermi theory. At even higher pressures and temperatures, the effect of radiation becomes crucial, because in this range of parameters, the contribution of the energy and pressure of the equilibrium light radiation is predominant for the system thermodynamics and, hence, the system dynamic mode close to the radiation – gas dynamic mode is realized.

The physical and chemical events that arise in a substance are illustrated by Fig. 14. The situation depicted on the left corresponds to a relatively low density where the substance can be represented as a rarefied gas composed of weakly interacting particles. In this case, it is possible to describe the particle interaction cross-sections, determine the equilibrium constants of the occurring transformations and follow the development of one or another process. If the substance is compressed, the situation shown on the right is realized — a close atom packing is formed. From the theoretical standpoint, this is a very inconvenient object. It is impossible to distinguish any single cell, and a typical multicentre problem appears where electrons belong simultaneously to an assembly of neighbours. Hence, the perturbation theory methods and other methods are not suited for the description of a highly compressed and heated substance. Under these conditions, electrons are collectivized and are free to move over the substance, which thus passes to the highly conductive 'metallic' state. This pronounced effect crucially changes the chemical processes in this medium. Under laboratory conditions using modern technology (see below), any dielectric can be brought to the metallic state and for any compound, it is possible to determine the pressure and temperature where this transition take place (*i.e.*, where the outer electron shells overlap).

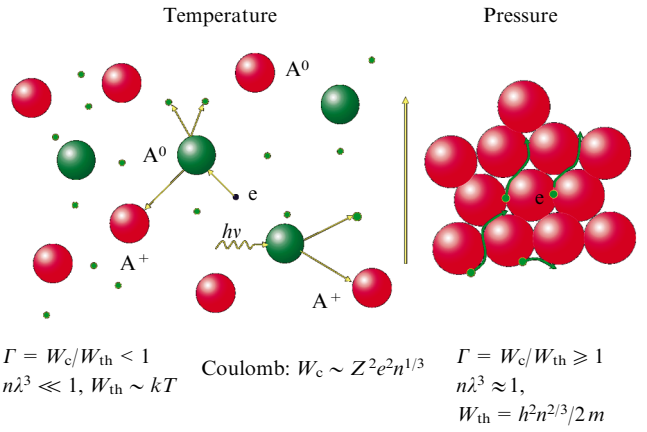


Figure 14. Schematic of temperature- and pressure-induced ionization.
Γ is non-ideality parameter, W_c is the average Coulomb interaction energy, W_{th} is the average thermal energy, n is the density of particles, λ is de Broglie wavelength, h is the Plank's constant, m is the particle mass.

Electrical conductivity is among the most interesting and informative characteristics of the medium. Indeed, the electrical conductivity provides valuable information about elementary charge transfer processes[60] and, what is most important, about the equilibrium composition of plasma, because the transport current in partially ionized plasma is directly determined by the concentration of free charges. Here it is noteworthy that the charge separation into free and bound charges for non-ideal plasma is a complicated task in view of the strong interparticle interaction, which makes this separation not quite unambiguous. By measuring the electrical conductivity of non-ideal plasma, one can consider pressure-induced ionization, dramatic evidence for the interparticle interaction in compressed plasma.[4, 15, 25, 61 – 63]

It is known that a substance can be brought into the conducting state (ionized) by either heating or compression.[4, 60] Currently, the mechanism of temperature-induced ionization is the major and best studied mechanism in the plasma physics.[60] It is associated with heating of rarified plasma to a temperature comparable with the ionization potential of the substance ($T \sim J$). The pressure-induced ionization mechanism alternative to thermal ionization is associated with pronounced compression of a 'cold' substance to densities $n \sim a_0^{-3}$ sufficient for the overlap of atomic orbitals with the characteristic size of the Bohr radius.

$$a_0 \sim a_B = \frac{\hbar^2}{me^2}$$

For this criterion to be realized, it is necessary to advance to the condensed plasma density range and, as a consequence, to generate pressures in the megabar range. To separate these two ionization mechanisms in the experiment, it is necessary to perform 'cold' ($T \ll J$) compression of the substance by diminishing the thermal heating effects. Hydrogen proved to be the most appropriate subject for this purpose as its low molecular mass accounts for the lowest shock compression temperature.

Hydrogen is the most naturally abundant (90%) and simultaneously the simplest chemical element, which has been attracting attention of various researchers for almost 250 years. The vigorous studies of the equation of state and electrical conductivity are stimulated by the role of hydrogen plasma in the astrophysics and the physics of giant planets and by the search for high-temperature superconductivity of its metallic phase (Fig. 15). These are the

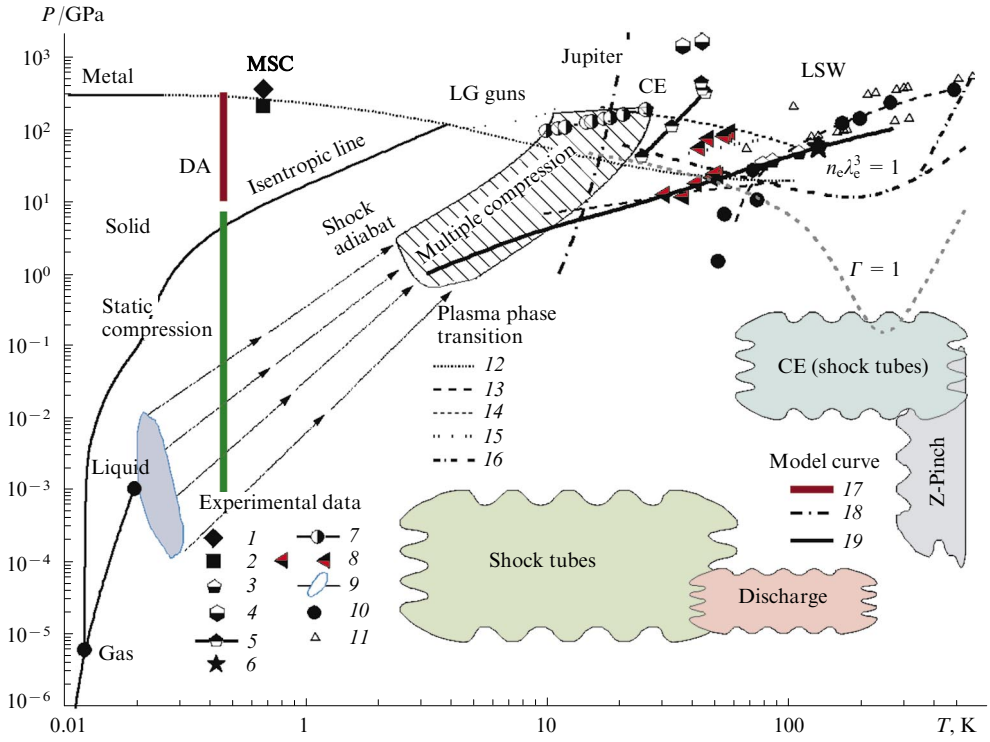


Figure 15. Phase diagram of hydrogen.[25]
Experimental data (for references to original sources, see Ref. 25): (*1*, *2*) magnetic compression; (*3*) Z-pinches; (*4*, *5*) cylindrical compression; (*6*) spherical compression; (*7*, *8*) single- and multiple-stage compression on a light-gas gun; (*9*) multiple shock compression; (*10*, *11*) laser radiation-induced shock compression. Estimates of the critical point of the hydrogen plasma phase transition: (*12*) Ebeling, (*13*) Robnik – Kundt, (*14*) Saumon – Chabrier, (*15*) Haronska, (*16*) Filinov. Experimental and theoretical data: (*17*) diamond anvil compression, (*18*) Jupiter atmosphere parameters, (*19*) adiabatic curves for hydrogen shock compression. DA are diamond anvils, LG guns are light-gas guns, LSW are laser shock waves, MSC is multiple shock compression.

permanent pragmatic incentives that promoted the research over the last 50 years.[64]

The pressure-induced ionization of hydrogen and noble gas plasmas was studied by multiple shock compression technique, which can accomplish quasi-adiabatic compression with a considerable ($\sim$10-fold) increase in the compression ratio and a decrease [to $(4-5)\times10^3$ K] in the substance temperature.[15, 25, 26, 40, 61, 65] The experiments were carried out in planar and cylindrical geometry using light-gas guns and explosion launching devices and cylindrical magnetic cumulation explosion generators[28, 29] in which high-intensity magnetic field is used to render the process isentropic.

Numerous experiments revealed a sharp (by up to 5 – 6 orders of magnitude) increase in the static electrical conductivity of hydrogen in a narrow range of condensed density at megabar pressures (Fig. 16). The highest electrical conductivity level achieved under these conditions is about several hundred $\Omega^{-1}\,cm^{-1}$; this is close to the electrical conductivity of alkali metals and is comparable with the Ioffe – Regel 'minimum metallic' conductivity.[66] In this connection, the effect in question is often called 'metallization', which of course is not quite correct, because according to publications,[66, 67] the notions 'metal' and 'dielectric' can be separated only at $T = 0$ K. In our opinion, in the given case, one deals with pressure-induced ionization[25, 62] caused by the overlap of the wave functions of neighbouring atoms, which facilitates the ionization in the dense medium. Figure 17 presents the geometric characteristics of an isolated hydrogen molecule in comparison with the available space per molecule (Wigner – Seitz cell radius) at a chosen density ρ. It can be seen that for the density $\rho > 0.3$ g cm^{-3}, hydrogen molecules become comparable to and then smaller than the Wigner – Seitz sphere size. Physically, this corresponds to pronounced overlap of the electron wave functions of neighbouring atoms even in the ground energy state. This overlap creates conditions for delocalization of electrons,[66] which, hence, are quasi-free to move in plasma. The energy spectrum and the effective ionization potential of hydrogen (ΔE) as a function of the Wigner – Seiz sphere size are given in Fig. 18. The red lines designate the lower edge of the band calculated assuming that the radial part of the wave function $R_{nl}(r_s)$ is equal to zero at the cell boundary, while the blue lower edge of the band was determined from a similar condition for the wave function derivative $R'_{nl}(r_s) = 0$ (for details, see Ref. 25). It can be seen that during compression (decrease in r_s), the energy levels are broadened and transform into energy bands, then these bands overlap and, as a consequence, the effective ionization potential of the substance decreases. The ΔE value obtained in this way is in reasonable agreement with the corresponding value found from experimental measurements of the temperature dependence of conductivity.

Similar conductivity data for quasi-adiabatic compressed plasma were obtained fort some other elements:

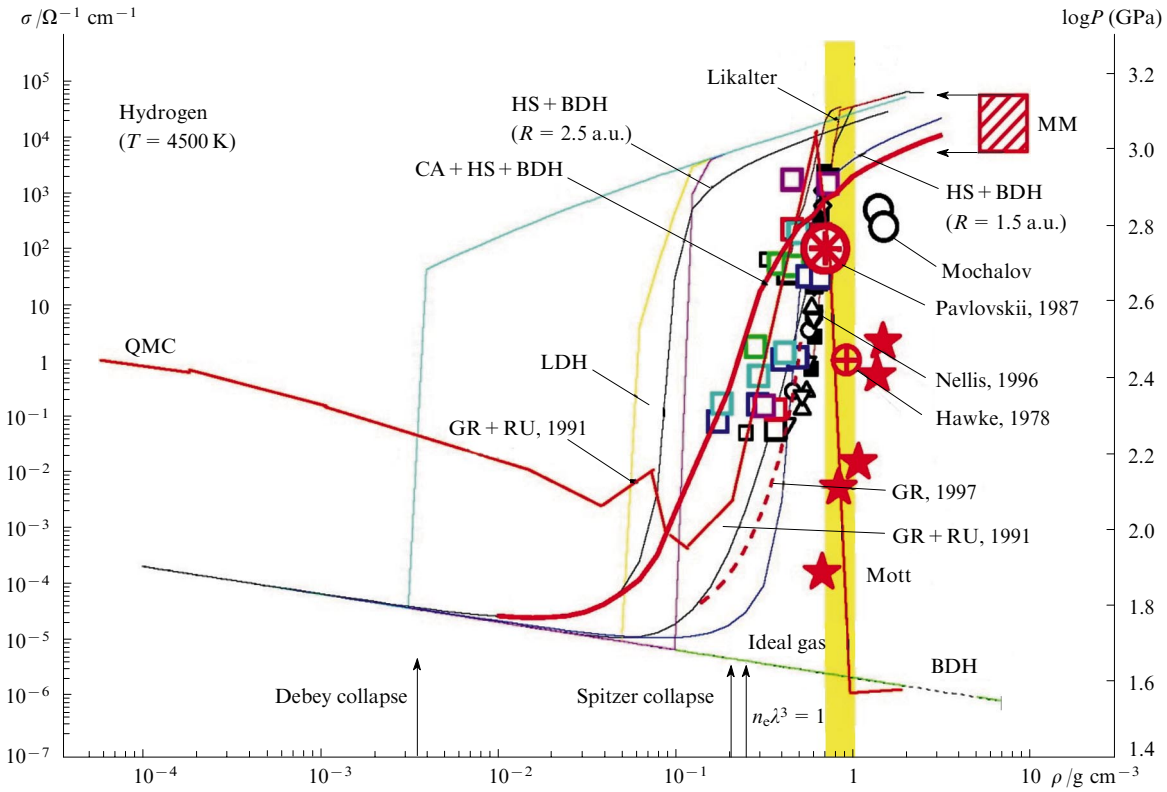


Figure 16. Pressure ionization of non-ideal hydrogen plasma.[15, 25, 26, 40, 61, 65]
Yellow marks the domain of thermodynamic phase transition, stars shows the results of density by pulsed X-ray radiography measurements,[26, 65] QMC are quantum Monte Carlo calculations.[68, 69] Theoretical models (for details, see Refs 1 and 25): BDH is the Debye approximation in a grand canonical ensemble for the ionization equilibrium; HS + BDH (R = 2.5 a.u.) is the Debye approximation in a grand canonical ensemble for the ionization equilibrium and the hard sphere model for heavy particles with the sphere radius R = 2.5 a.u.; CA + HS + BDH is the Debye approximation in a grand canonical ensemble for the ionization equilibrium and the hard sphere model for heavy particles with the sphere radius calculated in terms of the 'confined atom' model; GR is the Debye approximation in a grand canonical ensemble for the ionization equilibrium with the Coulomb interaction determined by the SAHA model; GR + RU is the Debye approximation in a grand canonical ensemble for the ionization equilibrium with the Coulomb interaction determined by the SAHA model and the particle size considered in terms of virial expansion; LDH is the Debye approximation in a small canonical ensemble; MM is the minimum metallic conductivity.

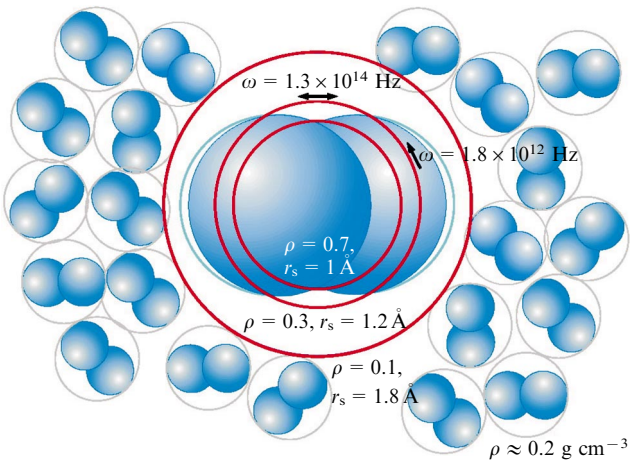


Figure 17. Hydrogen molecule in the megabar pressure range.[15, 25, 26, 40, 61, 65]
r_s is the Wigner – Seitz cell size at the density ρ.

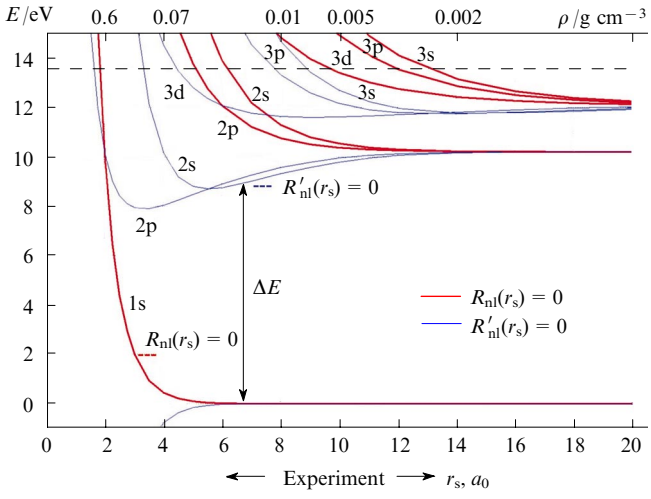


Figure 18. Energy spectrum of compressed hydrogen as a function of the Wigner – Seitz sphere size.[25]
$R_{nl}(r_s)$ and $R'_{nl}(r_s)$ is the radial wave function and its derivative.

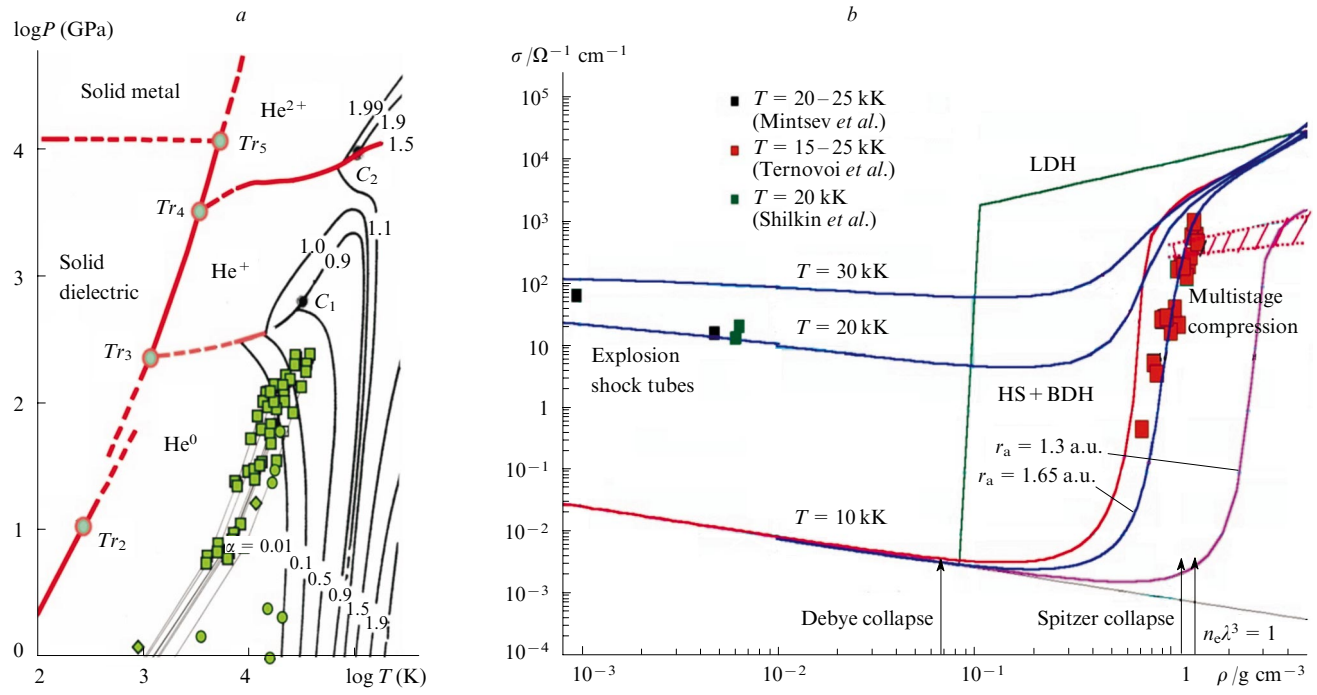


Figure 19. Phase diagram (*a*) and pressure-induced ionization of the helium plasma (*b*).[25]
C_i are critical points, Tr_i are triple points, α is the degree of ionization, r_a is the sphere radius in the model of Refs 25 and 30.

helium (Fig. 19), deuterium, argon, xenon and a hydrogen–helium mixture — plasma in the Jupiter atmosphere.[25]

The effects of overlap of electron shells were additionally studied in experiments[70] on quasi-adiabatic compression of C_{60} fullerene with the characteristic size of the molecule substantially exceeding the size of the hydrogen atom (7 Å *versus* 1 Å). As expected, the pressure of 'metallization' of C_{60} fullerene (Fig. 20) was approximately an order of magnitude lower than that of hydrogen.

Yet another interesting example is the compression of the alane molecule comprising a relatively large atom, aluminium, bonded to hydrogen atoms (AlH_3). In this case, so-called chemical compression is considered.[71] The pressure of substance 'metallization' is not high (~50–90 GPa), being determined by the small size of the hydrogen atom and relatively short distances between the neighbouring atoms, so that their electron shells can overlap (Fig. 21). The dependence of the electrical conductivity on the partial volume of hydrogen demonstrates good agreement of the density of the onset of sharp increase in the electrical conductivity and hydrogen 'metallization' (Fig. 22).

Note that the Mott, Anderson, Lifshitz, Herzfeld and Likalter models of transition of a substance to the conductive state (for details, see Refs 25 and 66) also predict transitions in the range of parameters close to the experimental range.

A characteristic feature of most physical models of non-ideal plasma is their thermodynamic instability in the region of high non-ideality parameters $\Gamma > 1$,[62,68,69,72–79] *i.e.*, where dynamic plasma compression experiments were planned and performed.[15,25,26,40,61,65] The instability of highly compressed Coulomb systems corresponds to the 'plasma' phase transition predicted, using simplified models, by Wigner,[72,73] Zel'dovich and Landau,[67] Norman and Starostin,[74] Ebeling *et al.*[62,66] and Saumon and Chabrier,[75,78] and reproduced by molecular dynamics[79] and quantum Monte Carlo methods.[68,69] The corresponding plasma instability domain (Debye collapse) predicted by the Debye ring approximation is marked in Fig. 19 *b* by the left vertical arrow. Monte Carlo calculations of the structure of non-ideal hydrogen plasma using path integral technique to take into account quantum effects were reported.[68,69] Phase separation with the subsequent formation of an ordered structure in non-ideal plasma can be clearly seen.

Here, apparently, it is pertinent to note the general tendency of highly compressed Coulomb systems to spatial ordering — the phase transition giving plasma liquids and crystals. To date, Coulomb crystals of this type have been observed in some exotic experimental situations: in non-ideal 'dust'[80] and colloid[81] plasma, in ion bunches cooled by laser radiation in electrostatic traps[82] and cyclotron accelerators[83] and in two-dimensional electron gas on a liquid helium surface.[66,84]

In the search for the phase transition in a real electrically neutral electron–ion plasma, experiments were carried out[26,65] dealing with quasi-adiabatic explosion compression in the cylindrical geometry of a deuterium plasma with plasma density measurement by pulsed X-ray radiography (see Fig. 3). The experimental results showed a sharp (~25%) jump of the plasma density at ~1.2 Mbar, just in the range of parameters where electrophysical measurements[15,25,26,40,61,65] clearly demonstrate a sharp (by 5–6 orders of magnitude) increase in the electrical conductivity (Fig. 23), while Monte Carlo calculations[68,69] lose their stability. The non-ideality parameters estimated for these

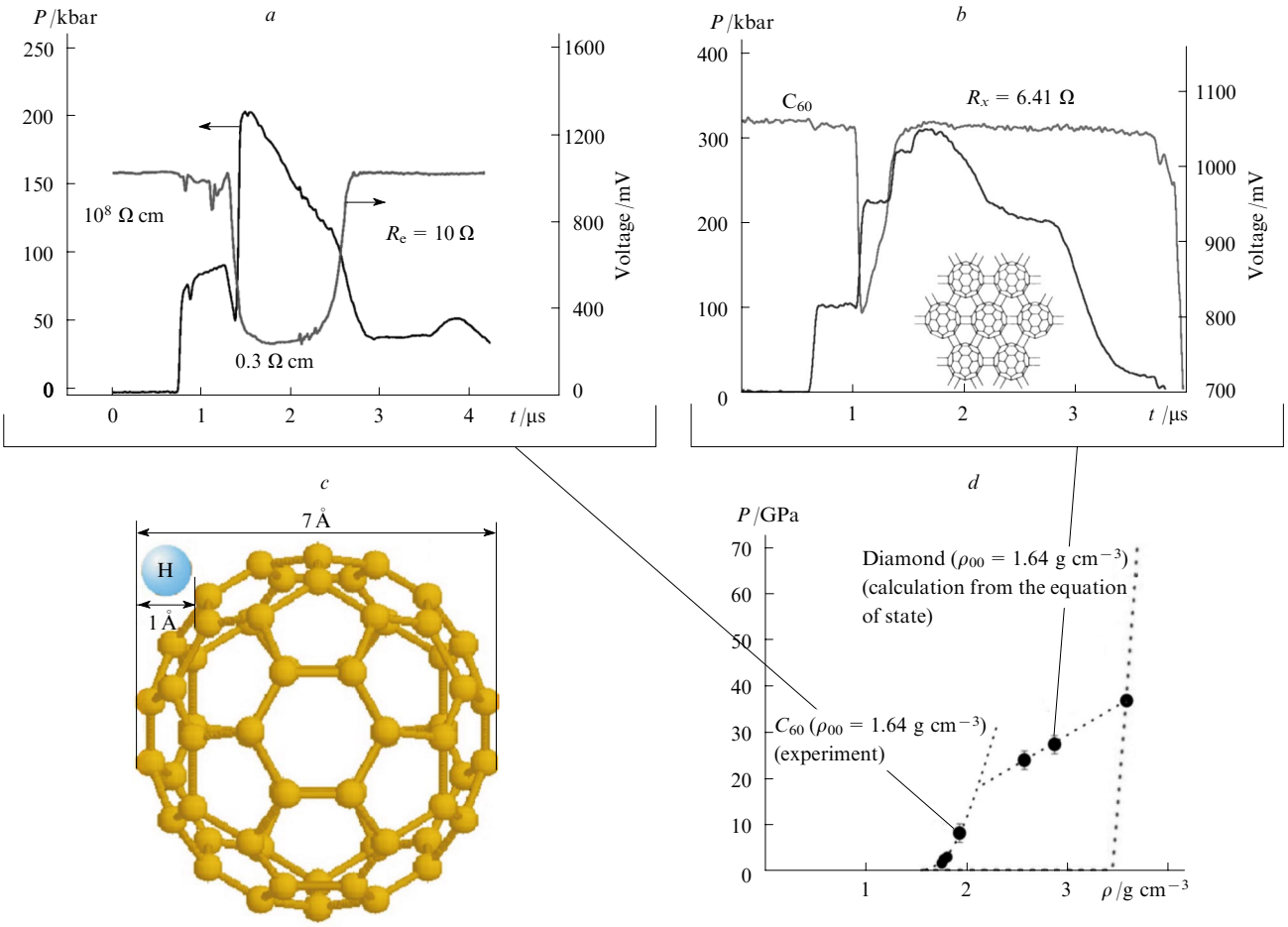


Figure 20. 'Metallization' of C_{60} fullerene at high dynamic pressures.[70]
(*a*, *b*) Experimental dependences of pressure and resistivity on the time at different compression intensities; (*c*) characteristic parameters of fullerene; (*d*) phase diagram of carbon; R_e and R_x are the shunt resistances in the measuring circuit.

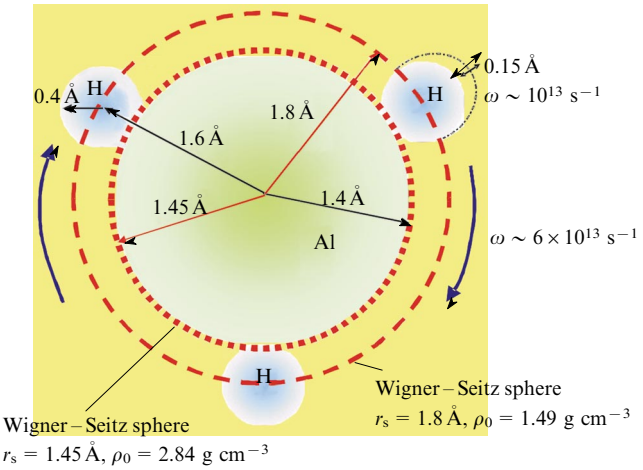


Figure 21. Chemical compression. Structure of the AlH_3 molecule.[71]

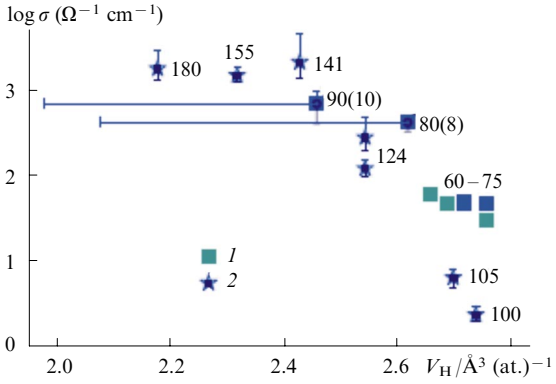


Figure 22. Electrical conductivity of alane *vs.* the partial volume of hydrogen.[71]
(*1*) Alane, (*2*) hydrogen; the numbers near the points are the compression pressures (GPa); the numbers in parentheses show the accuracy of pressure determination.

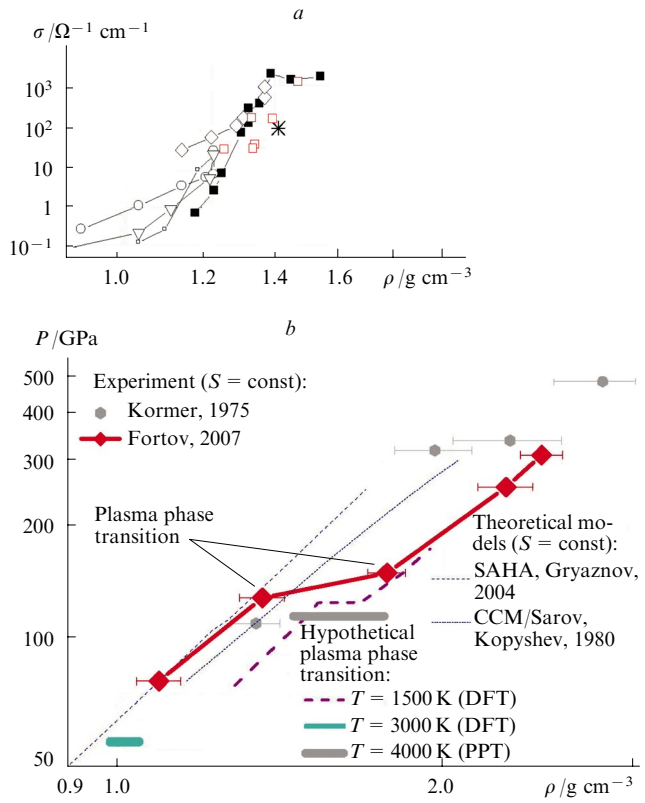


Figure 23. Variation of the electrical conductivity (*a*) and detection of the adiabatic compressibility of deuterium plasma (*b*).[25, 65]
DFT is the density functional theory, PPT is the plasma phase transition.

conditions are $\Gamma \approx 150-200$ with partial plasma degeneracy $n\lambda^3 \approx 1$.

Presumably, the thermodynamic and electrophysical measurements attest to experimental detection of a phase transition in non-ideal plasma upon multiple shock compression.

The temperature ionization of dense plasma was studied in experiments on shock-wave compression of heavy inert gases; due to high molecular mass, they are especially efficiently heated in shock waves. The experimental Coulomb (caused by electron scattering from charges) component of the static electrical conductivity of plasma in the dimensionless form

$$\sigma^* = \sigma\omega_p^{-1},$$

where

$$\omega_p = \sqrt{\frac{4\pi e^2 n_e^2}{m}}$$

is the Langmuir frequency, is shown in Fig. 24. It can be seen that the experiment covers a broad range of parameters including the high-density region (up to 3 g cm^{-3}) and plasma non-ideality values $\Gamma > 10$. In this range, the existing electrical conductivity models produce unphysical results (Spitzer and Coulomb divergences) caused by overestimation of the Coulomb scattering and screening effects.[4, 25, 85, 86]

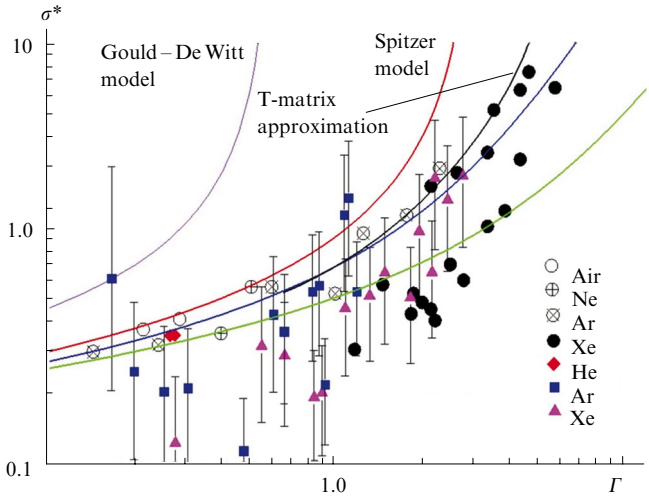


Figure 24. Temperature ionization $T \sim J$.[85, 86]
Static electrical conductivity of non-ideal plasma.

Subsequently these electrical conductivity measurements were supplemented by fairly useful measurements of the Hall conductivity of shock-compressed plasma[87] in a longitudinal magnetic field, resulting in determination of the carrier concentration, as this is commonly done in the semiconductor technology[66] (Fig. 25).

Measurements of resonance laser radiation reflection from shock-compressed plasma[88, 89] provide independent information about the number of free electrons and the frequency of electron collisions and thus serve for indirect verification of the models of plasma ionization and scattering in non-ideal plasma. The data shown in Fig. 26 indicate

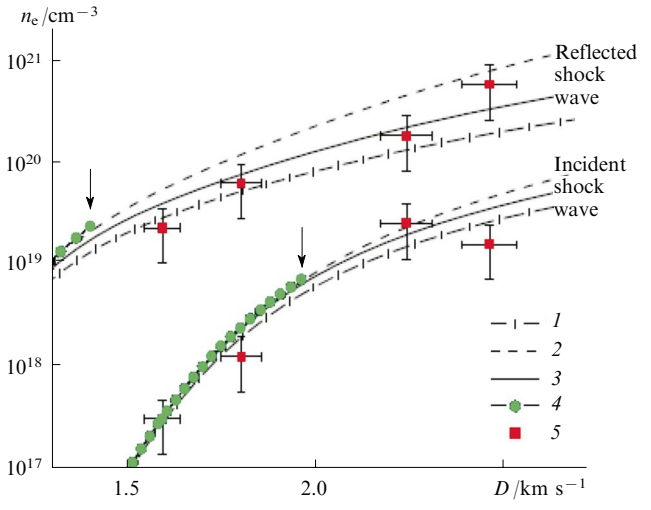


Figure 25. Density of electrons of xenon plasma (n_e) *vs.* the velocity of incident shock wave (D) from the results of Hall conductivity measurements.[87]
Calculations: (*1*) in the ideal plasma approximation, (*2*) in the ring approximation in grand canonical ensemble, (*3*) in the Debye approximation in grand canonical ensemble, (*4*) by the Debye – Hückel model, (*5*) experimental data. The arrows point to the divergence of Debye – Hückel calculations.

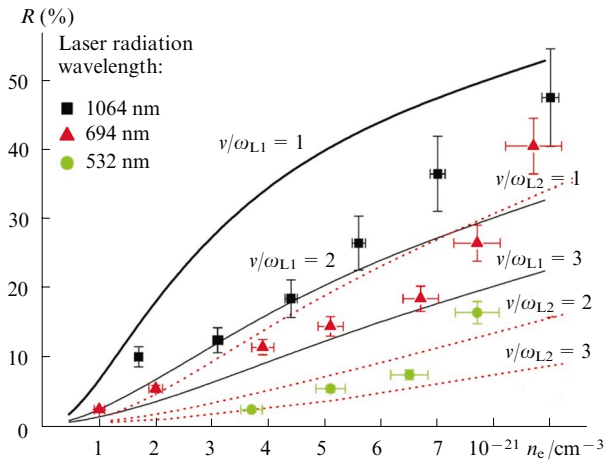


Figure 26. Curves for coefficients of reflection (R) of laser light *vs.* the shock-compressed plasma front.[89]
ν/ω_{Li} is the ratio of the frequency of electron collisions to the laser radiation frequency.

that the plasma reflection coefficient increases with increase in the plasma density to reach high values characteristic of metallic mirrors.

The measurements of optical properties of highly compressed plasma also gave quite unexpected results. According to the views developed for non-ideal plasma,[60] a density increase is expected to increase the opacity due to a broadening of spectral lines and a shift of the bremsstrahlung continuum. However, experimental data demonstrated[4,90] that in some cases, the broadening effects are less pronounced and the highly excited states themselves may be absent from the observed spectra. The reason is that the strong interparticle interaction in non-ideal plasma induces a shift, broadening and 'dissolution' of spectral lines, as indicated by the observed emission spectra of hydrogen, argon (Fig. 27), aluminium and xenon plasma.[91] The confined atom model partially describes these subtle effects.

According to this model,[4,25] plasma is treated as an equilibrium mixture of electrons, ions and neutral particles, their internal electronic structure being calculated by the Hartree–Fock method, which is suitable under appropriate conditions for the calculation of the wave functions and the energy levels and, after that, also the corresponding oscillator strengths of spectral lines and excitation and ionization cross-sections.[25,81] An example of calculations of this type for argon plasma is given in Fig. 27 where one can clearly see the 'collapsing' of energy levels upon plasma compression, resulting in 'transparentization' of dense plasma.

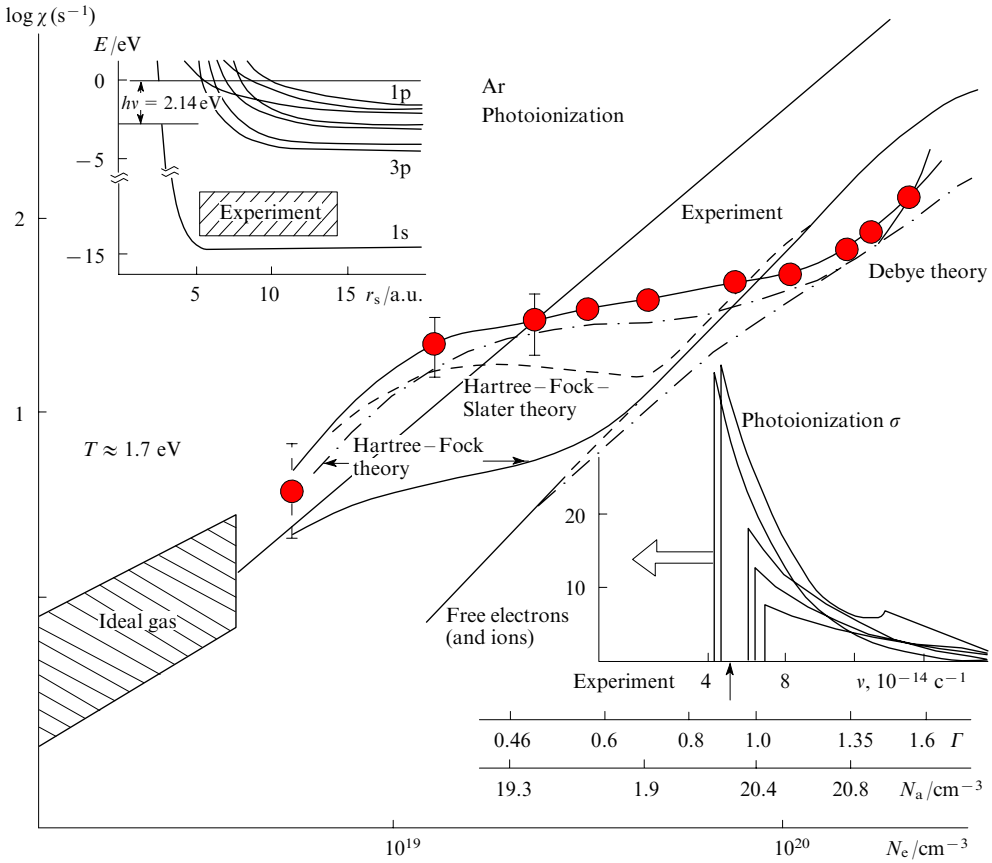


Figure 27. Results of calculations and measurements of the optical properties of compressed argon plasma demonstrating the effect of plasma 'transparentization'.[90]
χ is the absorption coefficient, ν is the radiation frequency, N_e is the concentration of electrons, N_a is the concentration of atoms.

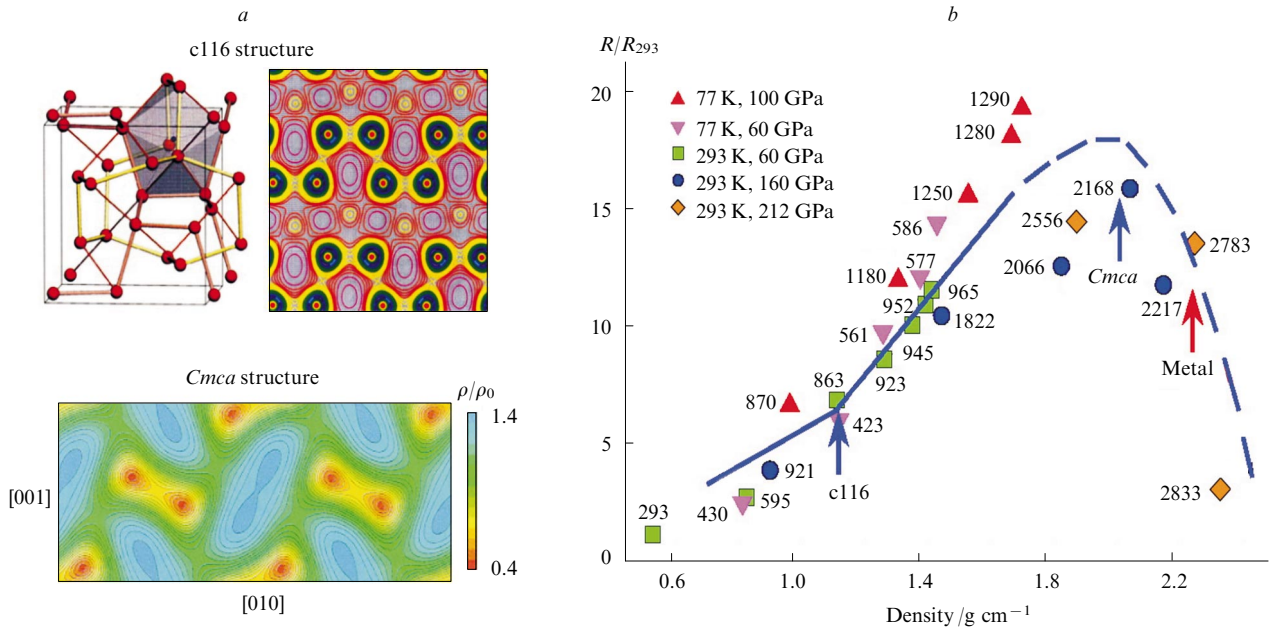


Figure 28. Structure and electron density distribution for high-pressure phase (*a*)[93] and pressure-induced 'dielectrization' of degenerate lithium plasma (*b*).[39]
The arrows indicate the breaks of conductivity, which are attributed to the appearance of a new (indicated nearby) phase and metallic conductivity; the numerals near the dots are calculated temperatures.

The shock-wave compression of 'ordinary' metals[92] revealed a remarkable behaviour of the degenerate strongly non-ideal plasma in the megabar pressure range.[27, 92, 93] According to the views existing until now,[66] the electronic properties of alkali metals are described by the simple model of uniform electron Fermi gas with point ions being located inside. However, modern quantum mechanical models[23, 93] predict the formation at elevated pressures (0.3 to 1.0 Mbar) of intricate crystal structures with high coordination numbers in which the conduction electrons are paired and, consequently, the conductivity decreases. Experiments on Li, Na and Ca quasi-adiabatic compression in this dynamic pressure range[23, 39, 92] steadily demonstrate this unusual effect, pressure-induced 'dielectrization' of ordinary metals[23, 39, 92] (Fig. 28). It can be seen that compression results first in a increase in the lithium resistivity, and hence, a decrease in the metal conductivity ('dielectrization'), while starting from 1.2 – 2 Mbar, the metal switches again to the metallic state, which will probably be fully retained during further compression.

Studies by advanced techniques of quantum chemistry revealed an unexpected pattern of structural transformation of matter following pressure increase. Just several years ago it was believed that the phase diagram of a substance is rather simple: as pressure increases, the substance transforms into more and more dense structures, dielectrics finally turn into metals, and the position of the melting curve obeys the Lindemann law. However, recent density functional theory calculations showed that inner electrons have a pronounced effect on the phase diagram appearance. In relation to lithium (Fig. 29), it can be seen that at higher pressure new phases appear, *i.e.*, the following transformations take place

$$\text{BCC} \longrightarrow \text{FCC} \longrightarrow \text{c116} \longrightarrow \textit{Cmca}24 \longrightarrow P\,432,$$

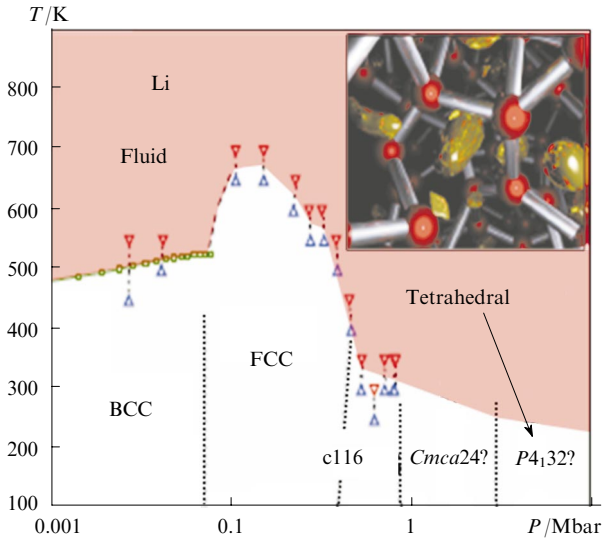


Figure 29. Phase diagram of lithium.[94]

and the melting curve acquires an unexpected form with negative dT/dP values in the megabar pressure range. Calculations of the aluminium structure[95] indicated (Fig. 30) that at higher pressures, the structure transforms into several phases, and at ~100 Mbar, unusual CMMA Electride structure, which crucially differs from usual dense structures, becomes stable for aluminium.

Calculations of the structures arising during compression of dielectrics, including the 'metallization' region, also show their unusual properties. In the ammonium structure, the type of bond changes upon compression. The *Pa*3

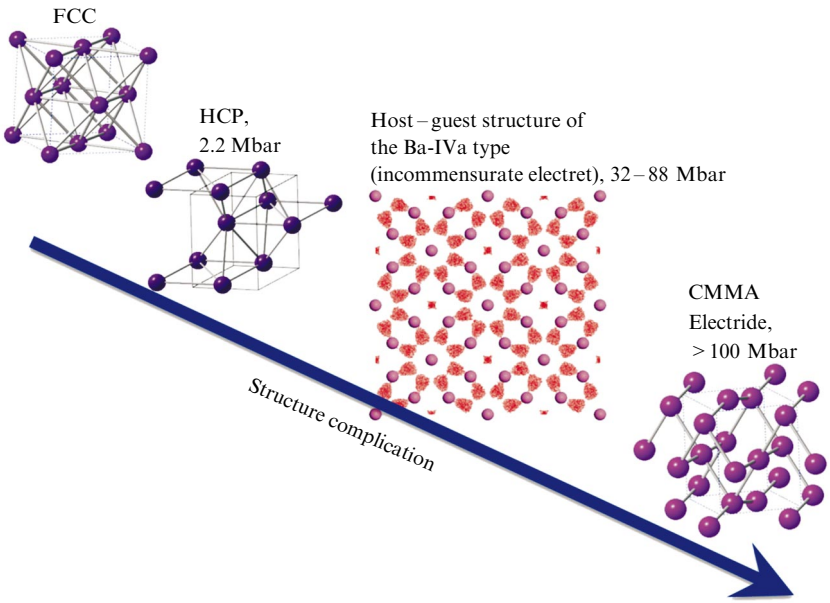


Figure 30. Structural transformation of aluminium with pressure increase.[95]

molecular structure found by calculations at ~5 GPa pressure[96] is transformed into an ionic crystal structure stable at >100 GPa.

Calculations of high-pressure phases for C, CO_2, N_2 and so on showed[97,98] that the liquid conducting phase is polymeric. The phase diagram of CO_2 reflects a great diversity of properties of some polymeric phases of this compound.[97] Of particular interest is polymeric nitrogen,[98–100] which is formed behind the front of intense shock waves or upon compression in diamond anvils at pressures >50 GPa and temperatures ~1500 K (Fig. 31). The reason is that if retained under usual conditions, this phase may be expected to exhibit unique detonation properties. Indeed, the nitrogen bond energy (E) is ~54 kJ g^{-1} for the density $\rho \approx 3.5$ g cm^{-3}, so polymeric nitrogen would be the most energetic chemical explosive, being an order of magnitude more powerful than well-known TNT ($E \approx 4.2$ kJ g^{-1} for $\rho \approx 1.6$ g cm^{-3}).

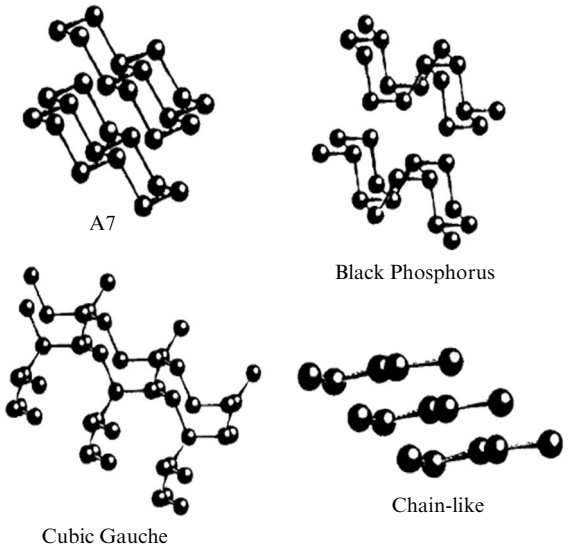


Figure 31. Structures of polymeric crystalline nitrogen.[99]

Finally, we approach the highest pressures where chemistry is expected to disappear. The data obtained from underground nuclear explosions demonstrate pressure-induced smoothing down of the specific atomic volumes of chemical elements (Fig. 32). Indeed, the sharp non-monotonicity of the dependence of the substance volume per nucleus (V_0) on the atomic number (Z) observed under normal conditions ($P = 0$) is due to the quantum nature of the material structure. This is fully reflected in the structure of the Periodic Table and chemical reactivity of elements. Compression leads to 'collapsing' and 'mixing' of electron shells, so that electrons lose their chemical uniqueness, their behaviour becoming more universal.[2] According to the experiment,[19] with increasing pressure the observed oscillations become less pronounced (the 1 and 10 Mbar curves), which supports the idea of 'simplification' of the substance structure and properties upon compression. Here the periodicity reflecting the shell structure of atoms is feebly manifested; hence, the specific chemical features of elements should also disappear. All neighbouring elements would have similar properties, which would be described by a quasi-classical approach to the self-consistent field method — the Thomas–Fermi theory.

However, record high energy densities in a substance under laboratory conditions are achieved upon frontal collision of heavy ions accelerated in synchrotron accelerators up to speeds near the speed of light.[101] These experiments are directed to the search for new particles,[102,103] experimental investigation of the fundamental problems of high-energy physics by hadron collisions, which give rise to the superdense nuclear matter, *viz*., quark-gluon plasma. Unique experiments on the generation of ultraextreme baryon matter in the superdense heated state with a density of ~10^{15} g cm^{-3}, pressure of 10^{30} bar and temperature of ~200 MeV upon single Cu–Cu and Au–Au heavy nucleus collisions were carried out at the CERN (Switzer-

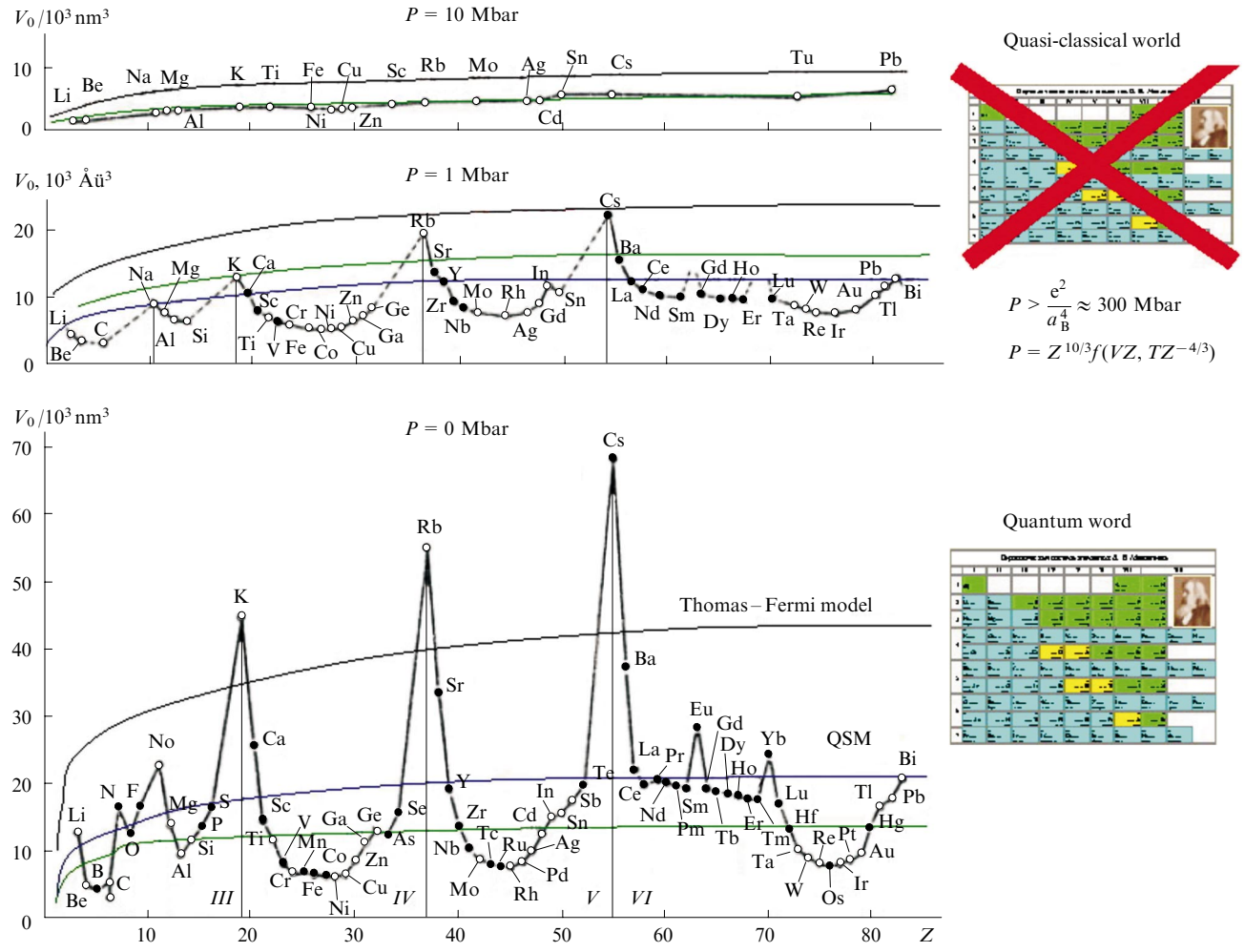


Figure 32. Change in the atomic volumes of elements with pressure increase.[19]
The shell effects diminish as pressure increases to become negligibly low at pressures of ~300 Mbar. At higher pressure, the substance properties become universal and their dependence on the atomic number becomes smooth and monotonic $P = Z^{10/3} f(VZ, TZ^{-4/3})$. The customary Mendeleev table, which determines positions of metals in the groups under usual conditions, is no longer valid, and the presented theoretical curves support this view.

land) and Brookhaven (USA) accelerators. Upon collision of two nuclei, the kinetic energy of movement transforms to the internal energy of nucleons, which, according to predictions of quantum chromodynamic theory,[103] gives rise to so-called 'colour glass condensate' and then, as thermalization occurs, to the new state of matter, quark-gluon plasma (quark soup).[103, 104]

Quark-gluon plasma arising upon such collisions consists of quarks, antiquarks and gluons.[105–107] The quark-gluon plasma has the maximum density of $\sim(9-10)\rho_0$ ($\rho_0 = 2.5 \times 10^{14}$ g cm^{-3} is the nuclear density); it may exist in the centres of neutron stars, black holes or upon the collapse of usual stars. Currently, large-scale experimental projects for the search for quark-gluon plasma have been initiated based on collisions of ultrarelativistic ions at the HERA and RHIC (Brookhaven), GSI (Darmstadt) and SPS and LHC accelerators (CERN). It is important that at these extreme densities, chemistry no longer exists, all processes being determined by interactions of fundamental particles.

* * *

Using shock waves generated by means of explosive chemical energy, it is possible to obtain, under laboratory conditions, states of matter with extremely high energy densities characteristic of the first seconds of Universe expansion after the Big Bang and states typical of astrophysical entities such as stars, giant planets and exoplanets.

The information gained in dynamic experiments substantially extends the fundamental views on the physicochemical properties of matter in a large domain of the phase diagram up to ultrahigh pressures, 10 orders of magnitude higher than the atmospheric pressure, and up to temperatures 7 orders of magnitude higher than the human body temperature.

In every intrusion into a new, previously unexplored area, the measured properties of matter prove to be fairly unusual and, as a rule, they strikingly contradict the concepts and models developed earlier. However, exactly this fact makes movement along the temperature and pressure

axes of state diagrams of substances especially fascinating and engrossing.

The authors considered only the small demesne of works in which they participated themselves. Much more information on the physics and chemistry of the extreme states of matter can be found in the cited publications.

References

1. V E Fortov *Ekstremal'nye Sostoyaniya Veshchestva* (Experimental States of Matter) (Moscow: Fizmatlit, 2009)
2. D A Kirzhnits *Usp. Fiz. Nauk* **104** 489 (1971) [a]
3. V E Fortov *Usp. Fiz. Nauk* **177** 347 (2007) [a]
4. V E Fortov, A G Khrapak, I T Yakubov *Fizika Neideal'noi Plazmy* (The Physics of Non-ideal Plasma) (Moscow: Fizmatlit, 2004)
5. *Frontiers in High Energy Density Physics* (Ed. D Henderson) (Washington, DC: National Research Council, National Academies Press, 2003)
6. V E Fortov *Usp. Fiz. Nauk* **138** 361 (1982) [a]
7. V B Mintsev, V E Fortov *Teplofiz. Vys. Temp.* **20** 745 (1982) [b]
8. S A Kaplan *Fizika Zvezd* (The Physics of Stars) (Moscow: Nauka, 1970)
9. S G Rubin *Ustroistvo Nashei Vselennoi* (Organization of Our Universe) (Fryazino: Vek-2, 2006)
10. A L Buchachenko *Khimiya kak Muzyka* (The Chemistry as Music) (Nobelistika, 2004)
11. R J Hemley, H K Mao, in *Proceedings International School of Physics 'Enrico Fermi'. Course CXLVII. High Pressure Phenomena* (Eds R J Hemley, G L Chiarotti) (Amsterdam, Oxford: JOS Press, 2002) p. 3
12. P Loubeyre, F Occelli, R Le Toulec *Nature (London)* **416** 613 (2002)
13. R Boehler *Nature (London)* **363** 534 (1993)
14. P Loubeyre, P M Celliers, D G Hicks, E Henry, A Dewaele, J Pasley, J Eggert, M Koenig, F Occelli, K M Lee, R Jeanloz, D Neely, A Benuzzi-Mounaix, D Bradley, M Bastea, S Moon, G W Collins *High Press. Res.* **24** 25 (2004)
15. W J Nellis *Rep. Prog. Phys.* **69** 1479 (2006)
16. E N Avrorin, B K Vodolaga, V A Simonenko, V E Fortov *Usp. Fiz. Nauk* **163** 1 (1993) [a]
17. L V Al'tshuler, K K Krupnikov, V E Fortov, A I Funtikov *Vestn. Ros. Akad. Nauk* **74** 1011 (2004) [c]
18. L V Al'tshuler, R F Trunin, V D Urlin, V E Fortov, A I Funtikov *Usp. Fiz. Nauk* **169** 323 (1999) [a]
19. L V Al'tshuler *Usp. Fiz. Nauk* **85** 199 (1965) [a]
20. Ya B Zel'dovich, Yu P Raizer *Fizika Udarnykh Voln i Vysokotemperaturnykh Gidrodinamicheskikh Yavlenii* (The Physics of Shock Waves and High-Temperature Hydrodynamic Phenomena) (Moscow: Nauka, 1966)
21. E N Avrorin, V A Simonenko, L I Shibashov *Usp. Fiz. Nauk* **176** 449 (2006) [a]
22. M V Zhernokletov, V N Zubarev, R F Trunin, V E Fortov *Eksperimental'nye Dannye po Udarnoi Szhimaemosti i Adiabaticheskomu Rasshireniyu Kondensirovannykh Veshchestv pri Vysokikh Plotnostyakh Energii* (Experimental Data on Shock Compressibility and Adiabatic Expansion of Condensed Substances at High Energy Densities) (Chernogolovka: Institute of Chemical Physics, Russian Academy of Sciences, 1996)
23. V L Ginzburg *O Fizike i Astrofizike* (About Physics and Astrophysics) (Moscow: Byuro Kvantum, 1995)
24. A V Zasov, K A Postnov *Obshchaya Astrofizika* (General Astrophysics) (Fryazino: Vek-2, 2006)
25. V E Fortov, V Ya Ternovoi, M A Zhernokletov, M A Mochalov, A L Mikhailov, A S Filimonov, A A Pyalling, V B Mintsev, V K Gryaznov, I L Iosilevskii *Zh. Eksp. Teor. Fiz.* **124** 288 (2003) [d]
26. V E Fortov, R I Ilkaev, V A Arinin, V V Burtzev, V A Golubev, I L Iosilevskiy, V V Khrustalev, A L Mikhaiov, M A Mochalov, V Y Ternovoi, M V Zhernokletov *Phys. Rev. Lett.* **99** 185001 (2007)
27. E G Maksimov, M V Magnitskaya, V E Fortov *Usp. Fiz. Nauk* **175** 793 (2005) [a]
28. R S Hawke, T J Burgess, D E Duerre *Phys. Rev. Lett.* **41** 994 (1978)
29. I Pavlovski, G V Boriskov, in *Megagauss Technology and Pulsed Power Applications* (New York, London: Plenum, 1987) p. 255
30. V K Gryaznov, M V Zhernokletov, I L Iosilevskii, G V Simakov, R F Trunin, L I Trusov, V E Fortov *Zh. Eksp. Teor. Fiz.* **114** 1241 (1998) [d]
31. V K Gryaznov, D N Nikolaev, V E Fortov *Khim. Fiz.* **17** 33 (1998) [e]
32. M V Zhernokletov *Teplofiz. Vys. Temp.* **36** 231 (1998) [b]
33. V E Fortov, I V Lomonosov *J. Pure Appl. Chem.* **69** 893 (1997)
34. L V Al'tshuler, R F Trunin, K K Krupnikov, N V Panov *Usp. Fiz. Nauk* **166** 575 (1996) [a]
35. R F Trunin *Usp. Fiz. Nauk* **164** 1215 (1994) [a]
36. G I Kanel, S V Rasorenov, V E Fortov *Shock-Wave Phenomena and Properties of Condensed Matter* (New York: Springer, 2004)
37. E I Zababakhin, I E Zababakhin *Yavleniya Neogranichennoi Kumulyatsii* (Phenomena of Inorganic Cumulation) (Moscow: Nauka, 1988)
38. S S Nabatov, A N Dremin, V I Postnov, V V Yakushev *Pis'ma Zh. Eksp. Teor. Fiz.* **29** 407 (1979) [f]
39. V E Fortov, V V Yakushev, K L Kagan, I V Lomonosov, V I Postnov, T I Yakusheva *Pis'ma Zh. Eksp. Teor. Fiz.* **70** 620 (1999) [f]
40. S K Grishechkin, S K Gruzdev, V K Gryaznov, M V Zhernokletov, R I Il'kaev, I L Iosilevskii, G N Kashintseva, S I Kirshanov, S F Manachkin, V B Mintsev, A L Mikhailov, A B Mezhevov, M A Mochalov, V E Fortov, V V Khrustalev, A N Shuikin, A A Yukhimchuk *Pis'ma Zh. Eksp. Teor. Fiz.* **80** 452 (2004) [f]
41. S I Belov, G V Boriskov, A I Bykov, R I Il'kaev, N B Luk'yanov, A Ya Matveev, O L Mikhailova, V D Selemir, G V Simakov, R F Trunin, I P Trusov, V D Urlin, V E Fortov, A N Shuikin *Pis'ma Zh. Eksp. Teor. Fiz.* **76** 508 (2002) [f]
42. G V Boriskov, A I Bykov, R I Il'kaev V D Selemir, G V Simakov, R F Trunin, V D Urlin, A N Shuikin, W J Nellis *Phys. Rev. B* **71** 092104 (2005)
43. L B Da Silva, P Celliers, G W Collins, K S Budil, N C Holmes, T W Barbee, B A Hammel, J D Kilkenny, R J Wallace, M Ross, R Cauble, A Ng, G Chiu *Phys. Rev. Lett.* **78** 483 (1997)
44. M D Knudson, D L Hanson, J E Bailey, C A Hall, J R Asay, W W Anderson *Phys. Rev. Lett.* **87** 225501 (2001)
45. V K Gryaznov, I L Iosilevskii, V E Fortov, in *Termodinamika Udarno-szhatoi Plazmy v Kvazikhimicheskom Predstavlenii. Termodinamicheskie Svoistva Nizkotemperaturnoi Plazmy. Prilozhenie k Entsiklopedii po Fizike Nizkotemperaturnoi Plazmy* (Thermodynamics of Shock-compressed Plasma in Quasichemical Repreentation. Thermodynamics Properties of Low-temperature Plasma. Appendix to Encyclopedia of Physics of Low-temperature Plasma) (Eds A N Starostin, I L Iosilevskii) (Moscow: Nauka, 2005) Vol. III-1, p. 111
46. O V Bazanov, V E Bespalov, A P Zharkov, V B Rumyantsev, T B Fedotova, V E Fortov, A L Misonochnikov *Teplofiz. Vys. Temp.* **23** 976 (1985) [b]
47. J R Turchi, W L Barker *J. Appl. Phys.* **44** 4936 (1973)
48. V A Gasilov, S V Zakharov, V P Smirnov *Pis'ma Zh. Eksp. Teor. Fiz.* **53** 83 (1991) [f]

49. E V Grabovskii, O Yu Vorob'ev, K S Dyabilin, A V Ostrik, V P Smirnov, V E Fortov *Pis'ma Zh. Eksp. Teor. Fiz.* **60** 3 (1994) [f]
50. A Pukhov *Rep. Progr. Phys.* **66** 47 (2003)
51. S I Anisimov, A M Prokhorov, V E Fortov *Usp. Fiz. Nauk* **142** 395 (1984) [a]
52. *Energy from Inertial Fusion* (Ed. W J Hogan) (Vienna: IAEA, 1995)
53. *Physics of High Energy Density* (Eds P Caldirola, H Knoepfel) (New York: Academic Press, 1971)
54. F F Chen *Introduction to Plasma Physics and Controlled Fusion* (New York: Plenum, 1984)
55. G A Mourou, T Tajima, S V Bulanov *Rev. Mod. Phys.* **78** 309 (2006)
56. B A Hammel *Plasma Phys. Controlled Fusion* **48** B497 (2006)
57. E I Moses, R E Bonanno, C A Haynam R L Kauffman, B J MacGowan, R W Patterson, R H Sawicki, B M Van Wonterghem *J. Phys. IV* **133** 57 (2006)
58. A S Vladimirov, N P Voloshin, V N Nogin, A V Petrovtsev, V A Simonenko *Pis'ma Zh. Eksp. Teor. Fiz.* **39** 69 (1984) [f]
59. R F Trunin, M A Podurets, G V Simakov, L V Popov, B N Moiseev *Zh. Eksp. Teor. Fiz.* **62** 1043 (1972) [d]
60. *Entsiklopediya Nizkotemperaturnoi Plazmy* (Encyclopedia of Low-Temperature Plasma) (Ed. V E Fortov) (Moscow: Nauka, 2000)
61. S T Weir, A C Mitchell, W J Nellis *Phys. Rev. Lett.* **76** 1860 (1996)
62. W Ebeling, A Foerster, V Fortov *Thermophysical Properties of Hot Dense Plasmas* (Berlin, Stuttgart: Teubner Verlagsgesellschaft, 1991)
63. V E Fortov, V K Gryaznov, V B Mintsev, V Y Ternovoi, I L Iosilevski, M V Zhernokletov, M A Mochalov *Contrib. Plasma Phys.* **41** 215 (2001)
64. E G Maksimov, Yu I Shilov *Usp. Fiz. Nauk* **169** 1223 (1999) [a]
65. M A Mochalov, M V Zhernokletov, in *Theses of International Conference on Strongly Coupled Coulomb Systems, Moscow, 2005* p. 35
66. V F Gantmakher *Elektrony v Razuporyadochennykh Sredakh (Kurs Lektsii)* [Electrons in Disordered Media (A Course of Lectures)] (Moscow: Nauka, 2005)
67. Ya B Zel'dovich, L D Landau *Zh. Eksp. Teor. Fiz.* **14** 32 (1944) [d]
68. V S Filinov, V E Fortov, M Bonitts, P R Levashov *Pis'ma Zh. Eksp. Teor. Fiz.* **74** 422 (2001) [f]
69. V S Filinov, P R Levashov, M Bonitz, V E Fortov *Plasma Phys. Rep.* **31** 700 (2005)
70. Yu A Osip'yan, B V Avdonin, K L Kagan, R K Nikolaev, V I Postnov, N S Sidorov, D V Shakhrai, A V Shestakov, V V Kveder, V E Fortov *Pis'ma Zh. Eksp. Teor. Fiz.* **81** 587 (2005) [f]
71. M Molodets, D V Shakhray, A G Khrapak, V E Fortov *Phys. Rev.* **79** 174108 (2009)
72. E Wigner *Phys. Rev.* **46** 1002 (1934)
73. E Wigner *Trans. Faraday Soc.* **34** 678 (1938)
74. G E Norman, A N Starostin *Teplofiz. Vys. Temp.* **8** 413 (1970) [b]
75. D Saumon, G Chabrier *Phys. Rev. Lett.* **62** 2397 (1989)
76. M Bonitz, I A Mulenko, E N Oleynikova, V S Filinov, V E Fortov, A L Khomkin *Plasma Phys. Rep.* **27** 1025 (2001)
77. W Ebeling, W Richert *Phys. Lett.* **108** (2) 80 (1985)
78. D Saumon, G Chabrier *Phys. Rev. A* **46** 2084 (1992)
79. M Baus, J P Hansen *Phys. Rep.* **59** 1 (1980)
80. V E Fortov, A V Ivlev, S A Khrapac, A G Khrapac, G E Morfill *Phys. Rep.* **421** 1 (2005)
81. W Jin, J P Reno, in *Strongly Coupled Plasma Physics* (Eds H Van Horn, S Ichimaru) (Rochester: University Rochester Press, 1993) p. 357
82. D H E Dubin, T M O'Neil *Rev. Mod. Phys.* **71** 87 (1999)
83. U Schramm, T Schatz, M Bussmann, D Habs *J. Phys., B* **36** 561 (2003)
84. A A Shashkin *Usp. Fiz. Nauk* **175** 139 (2005) [a]
85. V B Mintsev, V E Fortov, V K Gryaznov *Zh. Eksp. Teor. Fiz.* **79** 116 (1980) [d]
86. J R Adams, H Reinholz, R Redmer, V B Mintsev, N S Shilkin, V K Gryaznov *Phys. Rev. E* **76** 036405 (2007)
87. N S Shilkin, S V Dudin, S V Gryaznov, V B Mintsev, V E Fortov *Zh. Eksp. Teor. Fiz.* **124** 1030 (2003) [d]
88. V B Mintsev, Yu B Zaporogets *Contribut. Plasma Phys.* **29** 493 (1989)
89. H Reinholz, Yu Zaporoghets, V Mintsev, V Fortov, I Morozov, G Ropke *Phys. Rev. E* **68** 036403 (2003)
90. V E Fortov, V E Bespalov, M I Kulish, S I Kuz, in *Strongly Coupled Plasma Physics: Proceedings of the Yamada Conference XXIV* (Ed. S Ichimaru) (Amsterdam: Elsevier, 1990) p. 571
91. O V Denisov, N Yu Orlov, V E Fortov *Fiz. Plazmy* **27** 1081 (2001) [g]
92. V E Fortov, V V Yakushev, K L Kagan, I V Lomonosov, E G Maksimov, M V Magnitskaya, V I Postnov, T I Yakusheva *J. Phys.: Condens. Matter* **14** 10809 (2002)
93. J B Neaton, N W Ashcroft *Nature (London)* **400** 141 (1999)
94. I Tamblyn, J Raty, S Bonev *Phys. Rev. Lett.* **101** 075703 (2008)
95. C Pickard, R Needs *Nature Mater.* **9** 624 (2010)
96. G I G Griffiths, R J Needs, C J Pickard *Phys. Rev. B* **86** 144102 (2012)
97. B Boates, S Hamel, E Schwegler, S A Bonev *J. Chem. Phys.* **134** 064504 (2011)
98. B Boates, S A Bonev *Phys. Rev. B* **83** 174114 (2011)
99. A K McMahan, R LeSar *Phys. Rev. Lett.* **54** 1929 (1985)
100. R J Bartlett *Chem. Industry* (4) 140 (2000)
101. M Raiorden, U Zeits *V Mire Nauki* (8) 21 (2006)
102. K Kvig *V Mire Nauki* (5) 26 (2008)
103. S Mrowczynski, M H Thoma *Annu. Rev. Nuclear Part. Sci.* **57** (1) 61 (2007)
104. M Gyulassy, L McLerran *Nuclear Phys. A* **750** (1) 30 (2005)
105. D S Gorbunov, V A Rubakov *Vvedenie v Teoriyu Rannei Vselennoi. Teoriya Goryachego Bol'shogo Vzryva* (Introduction to the Theory of the Early Universe: Hot Big Bang Theory) (Moscow: LKI, 2008)
106. S Hands *J. Contempor. Phys.* **42** 209 (2001)
107. N K Glendenning *Compact Stars, Nuclear Physics, Particle Physics and General Relativity* (New York: Springer, 2000)

[a] — *Physics-Uspekhi (Engl. Transl.)*
[b] — *High Temper. (Engl. Transl.)*
[c] — *Herald Russ. Acad. Sci. (Engl. Transl.)*
[d] — *J. Exp. Theor. Phys. (Engl. Transl.)*
[e] — *Russ. J. Phys. Chem., Ser. B (Engl. Transl.)*
[f] — *J. Exp. Theor. Phys. Lett. (Engl. Transl.)*
[g] — *Plasma Phys. Rep. (Engl. Transl.)*